Université de Montréal

The effect of a VAChT-saporin immunotoxin on retinal cholinergic amacrine cells during post-natal development in rats

par

Manishha Patel

Sciences de la Vision
École d'Optométrie

Mémoire présenté à la Faculté des études supérieures
en vue de l'obtention du grade de
Maître es sciences (M.Sc.)
en Sciences de la Vision
option : Sciences fondamentales et appliquées

Mai 2005

Université de Montréal
Faculté des études supérieures

Cet mémoire intitulé:

The effect of a VAChT-saporin immunotoxin on retinal cholinergic amacrine cells during post-natal development in rats

Présenté par:

Manishha Patel

a été évalué par un jury composé des personnes suivantes:

Dr. Jean-François Bouchard, PhD
président-rapporteur

Dr. Christian Casanova, PhD
directeur de recherche

Dr. Maurice Ptito , PhD
membre du jury

FRENCH SUMMARY

Pour mon projet de maîtrise, j'ai étudié le rôle de l'acétylcholine rétinienne dans le développement du système visuel. Les cellules amacrines 'starburst' (AS) sont les seules cellules cholinergiques présentes dans la rétine et il a été démontré qu'elles étaient cruciales pour l'établissement de la sélectivité à la direction dans la rétine du lapin (Vaney et al, 1989). Chez le rat, néanmoins, le rôle de ces cellules dans l'établissement de la sélectivité à la direction n'a pas été clairement démontré.

Pour déterminer l'influence des cellules AS sur la sélectivité à la direction des neurones, nous avons injecté une immunotoxine (anti-VAChT:saporine) dans le vitré de rats nouveau-nés. Cette dernière est spécifiquement dirigée contre le transporteur vésiculaire de l'acétylcholine et devrait donc éliminer toutes les cellules cholinergiques amacrines de la rétine. Lorsque les rats attaiguent l'âge adulte, nous avons fait des enregistrements électrophysiologiques dans le colliculus supérieur (CS). Suite aux enregistrements, l'analyse immunohistochimique a démontré que seule la moitié des neurones cholinergiques était détruite. Nos résultats électrophysiologiques préliminaires suggéraient qu'il n'y avait pas de différence majeure dans les propriétés des champs récepteurs du CS, ce qui pourrait être dû à élimination partielle des cellules AS.

Nous sommes donc intéressés au développement des cellules AS, dans le but de déterminer à quel moment l'injection de notre toxine causerait une élimination complète de ces cellules. Nos injections, faites dans des rats d'âges différents (P0 à P60), ne permettent pas de conclure dû à l'inefficacité de la toxine immunologique.

FRENCH KEYWORDS

acétylcholine

cellule amacrine 'starburst'

collicule supérieur

développement

immunotoxine

rats

rétine

ENGLISH SUMMARY

This project investigates the role of retinal acetylcholine in neuronal development of the visual system. Starburst amacrine (SA) cells are the only cholinergic cells present in the retina and have been deemed crucial for direction selectivity in the rabbit retina (Vaney et al, 1989). In the rat, however, it is still unclear if SA cells are necessary for direction selectivity.

In order to determine the influence of SA neurons on direction selectivity, intravitreal injections of an immunotoxin (anti-VAChT:saporin) were carried out on rat pups. This toxin is specific for the vesicular acetylcholine transporter, and therefore should have eliminated all retinal cholinergic amacrine cells (Gunhan et al, 2002). When rats reached adulthood, electrophysiological recordings were done in the superior colliculus (SC). Following the recordings, immunohistochemistry was performed on the retinae of these animals. Interestingly, these retinae showed that only about 50% of cholinergic neurons were eliminated and preliminary results suggest that there was no major difference between normal and toxin-treated animals in terms of receptive field properties of the SC. This result could be attributed the partial elimination of SA cells.

Aiming to obtain the full elimination of SA cells, we then focused on determining the developmental course of SA cells, and when intravitreal injections of the immunotoxin would allow for complete elimination of SA cells from the retina. From the results of injections performed on rats of various age groups (P0 to P60), no conclusions could be made definitely from this part of the study since the immunotoxin was ineffective in eliminating any cholinergic neurons.

ENGLISH KEYWORDS

acetylcholine

development

immunotoxin

rats

retina

starburst amacrine cell

superior colliculus

TABLE OF CONTENTS

LIST OF TABLES

LIST OF FIGURES

LIST OF ABBREVIATIONS

ACh	acetylcholine
AchE	acetylcholinesterase
E	embryonic day
ChAT	choline acetylesterase
GABA	γ-aminobutyric acid
GC	ganglion cell
GCL	ganglion cell layer
INL	inner nuclear layer
IPL	inner plexiform layer
NM	neuromodulator
NT	neurotransmitter
ONL	outer nuclear layer
OPL	outer plexiform layer
P	postnatal day
SA	starburst amacrine
SC	superior colliculus
VAChT	vesicular acetylcholine transporter

Sic parvis magna

INTRODUCTION

1.1 The visual system

Vision is the most fundamental of our senses. It allows us to recognize visual cues from the world and respond appropriately. Although all parts of the eye are important for perceiving a good image, the most vital element for vision is the retina. The retina is essentially a piece of brain tissue that gets direct stimulation from the lights and images of the world. It translates the light into nerve signals and extracts useful information and ignores redundancies.

1.2 The retina

1.2.1 Structural organization and its development

The vertebrate retina is a laminated structure and is organized into five layers: two synaptic layers – inner and outer plexiform layers – which are interposed between three cellular layers – inner and outer nuclear layers and ganglion cell layer. In the temporal arrangement of the retina (Figure 1), the photoreceptors cell bodies are first in line and they are located in the outer nuclear layer. The inner nuclear layer contains the perikarya of horizontal cells at its outer margin; the majority of bipolar cell perikarya are found in the middle of the layer; and most amacrine cell perikarya are found along the proximal

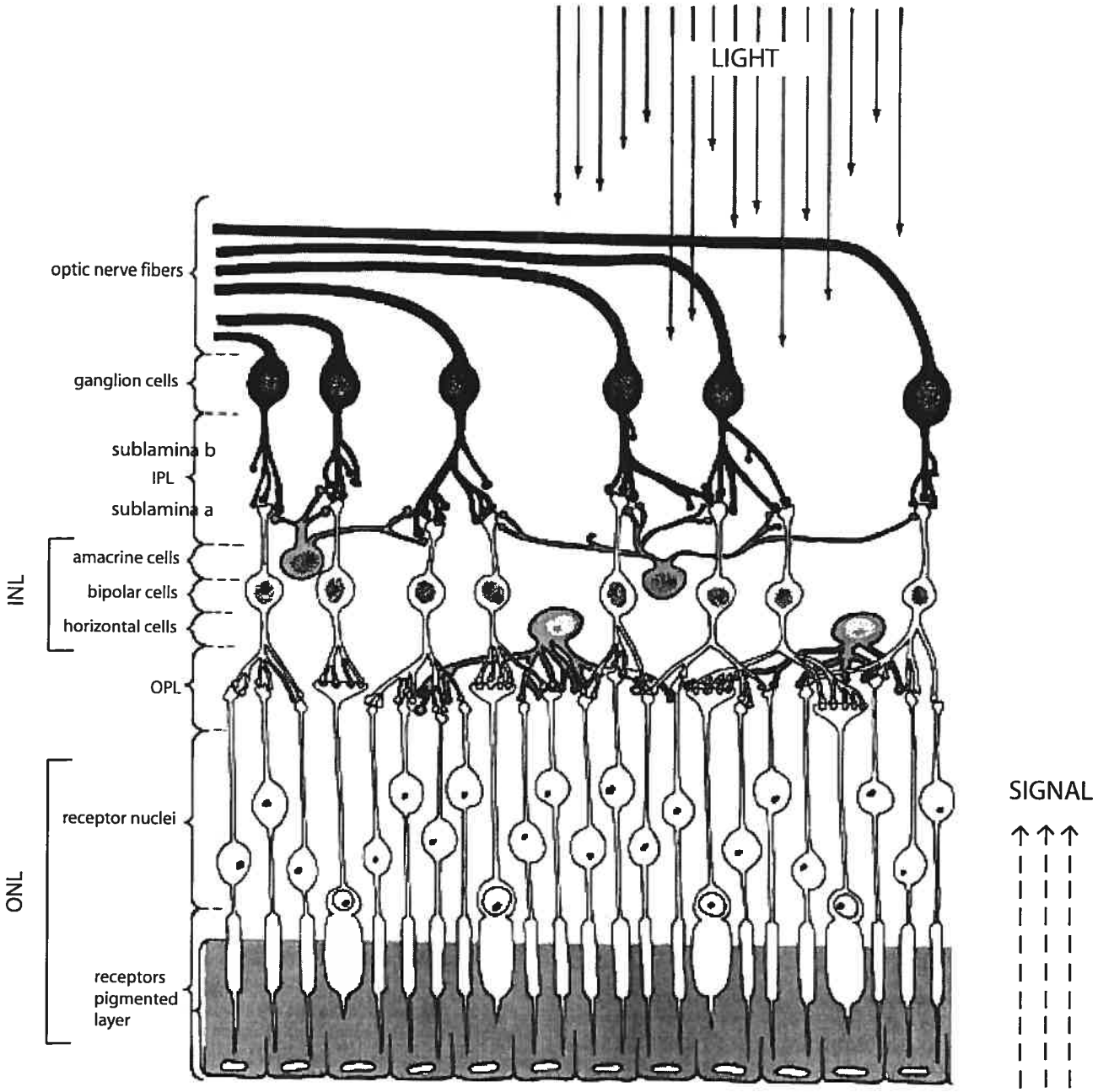

Figure 1: Illustration showing the cellular organization of a vertebrate retina. The solid-line black arrows show the direction in which light enters the eye. The dotted-line arrows indicate the direction in which information is conveyed once the light 'hits' the photoreceptors. INL: inner nuclear layer; IPL: inner plexiform layer; ONL: outer nuclear layer; OPL: outer plexiform layer. *From:* (Palmer, 1999).

border. The Muller cells are found throughout the retina, from the outer nuclear layer (ONL) to the inner margin of the retina. The outer plexiform layer (OPL) and inner plexiform layer (IPL) are areas where synapses are made between different cell types. The IPL is further divided into two regions – sublamina a, which is closer to the INL, and sublamina b, which is closer to the ganglion cell layer (GCL).

There are, however, exceptions to the aforementioned arrangement of the retina. Horizontal and bipolar cells may be found in the ONL, ganglion cells in the inner nuclear layer (INL), and amacrine cells in the GCL. These cells are named displaced cells. Displaced amacrine cells are a common feature of many retinae (Masland & Mills, 1979; Vaney, Peichi, & Boycott, 1981).

The retina is part of the central nervous system (CNS) and originates from the neural ectoderm during development. Groups of progenitors leave the cell cycle throughout retinal development to differentiate into one of seven cell classes (Carter-Dawson & LaVail, 1979; Sidman, 1961; Young, 1985b; Young, 1985a). Although there is considerable overlap between the generation periods of most cell classes, each retinal cell type is generated at a certain time point. Ganglion cells are the first neurons to be born, followed by amacrine, horizontal, cone photoreceptor cells, bipolar, and finally, Muller glial cells. Generation of rod photoreceptor cells can be seen almost throughout cytogenesis (Carter-Dawson et al., 1979; Sidman, 1961; Young, 1985b; Young, 1985a).

1.2.2 Developmental course of the rat retina

The retina is a derivative of the neural tube. The two optic vesicles develop very early in embryonic life and then invaginate to form the optic cups (Dowling, 1987b; Grun, 1982). It is the neural epithelium on the inner wall of the optic cups that eventually becomes the retina. Initially, both walls of the optic cup are one cell thick. These cells then divide to form a neuroepithelial layer many cells thick which then differentiate into all the retinal cells (Dowling, 1987b).

In the rat, mitoses occur in the scleral zone of the retina at the central and peripheral regions between embryonic day 9 (E9) and postnatal day (P13) (Rapaport, 2004), with the peripheral retina lagging behind the center by, on average, 1.9 days $\pm$ 11 hours. There is a decline in mitotic activity beginning approximately at P6, when ninety-five percent of all retinal cells have been generated. Cell genesis slows sharply for the production of the final five percent of cells (Rapaport, 2004).

Ganglion cells (GCs) are the first retinal cells to be born; labeling has been seen as early as E9 (Rapaport, 2004); ninety-five percent of these cells are present by E19. These are closely followed by horizontal and cone photoreceptor cells; first detected between E9 and E10 and ninety-five percent detected at E15/16 and E18, respectively. Next in line are the amacrine cells, which appear at E12 and are almost fully expressed by P7 (Rapaport, 2004). Rod photoreceptor genesis, starting at E18 and ending at approximately P13,

precedes a final cohort consisting of Muller and bipolar cells, which arise at E21 and are detected till P13 (Rapaport, 2004).

1.2.3 Functional organization and its development

The retina receives visual information that it segregates into two visual streams: one beginning with rod photoreceptors, and the other with cone photoreceptors. Rods are activated by dim-light conditions while cones function in bright light and are responsible for colour vision. The division between rod and cone vision allows for the extension of the range of illumination conditions under which we can see.

The first synapse in the retina is between photoreceptors and bipolar cells. Signals that represent local increments or decrements in luminance are separated into two pathways and carried off by ON (depolarizing) and OFF (hyperpolarizing) bipolar cells. These then synapse onto ganglion cells (Dowling, 1987a; Rodieck, 1998).

There are also lateral pathways involved in the visual stream. Figure 1 shows potential cell-to-cell interactions. In the OPL, there are horizontal cells that may influence the processing of visual information via its interactions with photoreceptors, bipolar cells, and with other horizontal cells (Haverkamp, Grunert, & Wassle, 2000; Vardi, Morigiwa, Wang, Shi, & Sterling, 1998). Another lateral pathway involves the amacrine cells located in the IPL. These

cells exert their effect by interacting with bipolar cells (Menger & Wassle, 2000) as well as with other amacrine cells.

1.2.3.1 Neurotransmitters and neuromodulators

In trying to understand the functional organization of the retina, questions arise about retinal synaptic mechanisms. The processing of visual information within the retina depends in large part on neurons interacting with each other via discrete and specific sites called synapses. Chemical messengers, either neurotransmitters (NTs) or neuromodulators (NMs) or both, relay information between cells and between different types of cells (Pycock, 1985; Daw, Brunken, & Parkinson, 1989).

There are over a dozen proven or presumed NT chemicals identified in the mammalian retina. Each cell type in the retina has usually been correlated with one or more NT(s) or NM(s); photoreceptors with glutamate, aspartate and taurine, horizontal cells with γ-aminobutyric acid (GABA), taurine, and glycine, GCs and bipolar cells with GABA and glutamate. However, the most chemically diverse cells in the entire retina are the amacrine cells; (Pourcho, 1996; Pycock, 1985) this is probably due to the diverse phenotypes of this group. Different types of amacrine cells include AI and AII cells, dopaminergic amacrine cells, and starburst amacrine cells. They participate in a variety of excitatory and inhibitory circuits in the IPL. In keeping with the diversity of function of these cells, many transmitter substances have been associated with

their pharmacology including acetylcholine (ACh), γ-aminobutyric acid (GABA), taurine, glycine, dopamine, and neuropeptides (ex. Substance P, somatostatin, vasoactive intestinal polypeptide) (Pycock, 1985).

1.3 Amacrine cells

Amacrine cells as a whole were first discovered in the late 1880's. The name 'amacrine' comes from the Greek *a-makrós-inos* meaning "without-long-fiber", so called by Ramon y Cajal in 1883. Since their discovery, a wide variety of subgroups have emerged based on morphology and pharmacology (Dowling, 1987a). As previously mentioned, this morphologically diverse group of cells is associated with a number of neurochemical agents and they are implicated in many inhibitory and excitatory circuits.

1.3.1 Starburst amacrine cells

Starburst amacrine (SA) cells are probably the best characterized of all amacrine cells. They have distinct characteristics that are found ubiquitously across species, suggesting a highly conserved role in the retina.

1.3.1.1 Characteristic properties of SA cells

SA cells have a distinctive radially symmetrical morphology where the primary dendrites are branched regularly and repeatedly, and are studded with varicosities. This gives the cells the appearance of starburst fireworks (Famiglietti, 1983) (Figure 2). There are two subpopulations of SA cells: one is located in the INL the other, forms a displaced population in the GCL. Both populations extend their dendrites into the IPL with the processes from the INL limited to sublamina a, and those from the GCL limited to sublamina b (Famiglietti, 1983; Voigt, 1986; Schmidt, Wassle, & Humphrey, 1985; Rodieck & Marshak, 1992). The density of these cells is greatest at the *area centralis* with a gradual decrease in number as we go towards the periphery, essentially mirroring the distribution of GCs (Schmidt et al., 1985; Vaney et al., 1981; Voigt, 1986; Rodieck et al., 1992).

1.3.2 Acetylcholine release by SA cells

ACh is one of the oldest and best understood NTs. It was first identified as a NT in the peripheral nervous system (Dale, 1914; 1935) and then in the central nervous system. Later studies showed that it is also a NT in the vertebrate retina (Neal, 1976). The synthesis and release of ACh is relatively

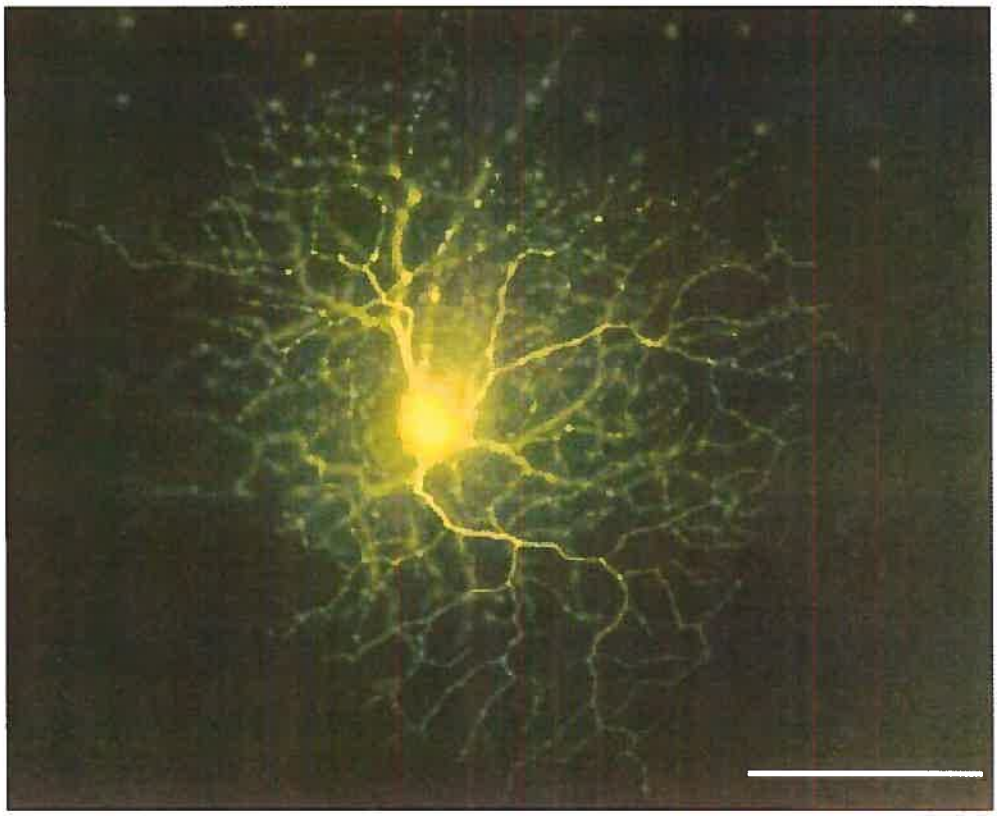

Figure 2: Image of a starburst amacrine cell from a rabbit retina labeled with Lucifer yellow. The dendrites are arranged radially around the cell body and are studded with varicosities. *From*: Masland (1986).

simple (Figure 3). It is synthesized in the cytoplasm from choline and acetyl co-enzyme A by the enzyme choline acetyltransferase (ChAT); this enzyme is contained only in cells that synthesize ACh and is therefore a marker enzyme that identifies cholinergic cells. Following synthesis, ACh is packaged into synaptic vesicles via the vesicular acetylcholine transporter (VAChT); a proton-dependent transporter. ACh is stored in these vesicles until its release from the presynaptic nerve terminal. After release, the ACh that is not taken up by the post-synaptic terminal is hydrolyzed by extracellular acetylcholinesterase (AChE) to yield choline and acetate. The choline is taken back up into the presynaptic neuron, and can be used to resynthesize ACh or to synthesize phospholipids, which can be used as stores of choline.

1.3.3 Implications in direction selectivity

Direction selectivity is the ability of a cell to interpret the direction of stimulus movement; there are many neurons in the visual system with this capability. The rabbit retina has been the focus of many studies on retinal direction selectivity because it contains direction selective ganglion cells. Most of the research has focused on the ON-OFF direction selective ganglion cells which make-up ten percent of the GCs in the rabbit retina (Vaney, 2001). There are four types of direction selective ganglion cells; each responds preferentially to image motion in one of the four cardinal ocular directions – upwards, downwards, forwards, and backwards (Oyster & Barlow, 1967). It appears that

Figure 3: Illustration depicting a cholinergic neuron. Diagrammed here, is the sequence of steps involved in the utilization of ACh as a NT. (1) Uptake of choline from the synaptic cleft by the presynaptic cell. (2) ACh is synthesized from choline and acetyl-coenzyme A (acetyl-SCo A) (acetate donor) by the enzyme choline acetyltransferase (ChAT). (3) Formation of a releasable pool of ACh. (4) Release of ACh from the presynaptic terminal. (5) Interaction of ACh with the postsynaptic cell. (6) Degradation of unused ACh by acetylcholinesterase (AChE) into choline and acetate.

From:

http://abdellab.sunderland.ac.uk/Lectures/Nurses/pics/cells/acetylcholine.jpg

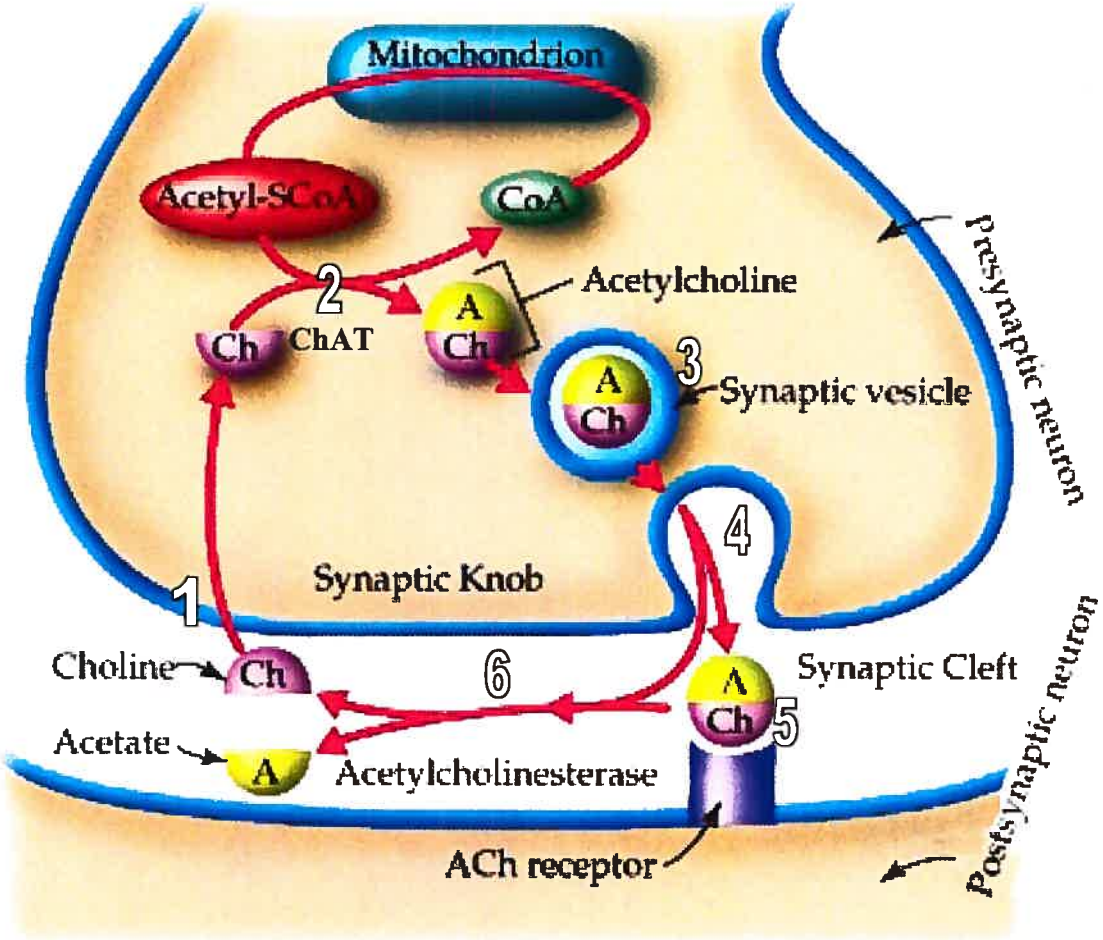
Mitochondrion
Acetyl-SCoA
CoA
2
Acetylcholine
A
Ch
Ch
ChAT
A
Ch
3
Synaptic vesicle
Presynaptic neuron
4
Synaptic Knob
1
Choline
Ch
6
A
Ch
5
Synaptic Cleft
Acetate
A
Acetylcholinesterase
ACh receptor
Postsynaptic neuron

each point on the retina is covered by the four different subtypes of direction selective ganglion cells whereas direction selective ganglion cells of the same subtype span the retina in a territorial manner with little overlap of their dendritic fields (Amthor & Oyster, 1995; Vaney, 1994).

There has been much debate on the locus of computation of direction selectivity. Taylor and colleagues (2000) argued that the direction selective ganglion cell is the first element to be fully direction selective in the rabbit retina while Borg-Graham (2001) argued that the first direction selective element is located somewhere earlier in the chain of synapses leading to the GC. To date, this conflict remains unresolved however, the latter theory has been extensively studied and the results are favourable.

One of the prime candidates for the laterally displaced element responsible for direction selectivity is the cholinergic SA cells. The ON- and OFF- SA cells stratify at precisely the same levels in the IPL as do the ON- and OFF direction selective ganglion cells (Famiglietti, 1987; Famiglietti, 1992) and within each stratum, the numerous overlapping processes co-fasciculate with those of the direction selective ganglion cells (Vaney & Pow, 2000; Tauchi & Masland, 1985).

SA cells receive bipolar and amacrine cell input over the whole dendritic tree, although their output to GCs is restricted to the varicose distal ends (Famiglietti, 1991). It is proposed that this proximodistal segregation of the output and input synapses supplies the spatial asymmetry required for the generation of direction selectivity assuming that dendrites on different sides of

SA cells provide selective output to direction selective GCs with different preferred directions (Vaney DI, 1989) (Figure 4). SA cells contain and release both acetylcholine (ACh), an excitatory NT and GABA, an inhibitory NT (Brecha, Johnson, Peichl, & Wassle, 1988; O'Malley, Sandell, & Masland, 1992; Vaney & Young, 1988). Due to this fact it is proposed that each direction selective GC would selectively receive from a SA cell, either a cholinergic input located on the preferred side of the GC, or a GABAergic input located on the null side. If the two mechanisms operated together in a push-pull fashion, a SA cell process pointing in one radial direction would selectively excite a direction selective GC with the same preferred direction and selectively inhibit an overlapping direction selective GC with an opposite preferred direction (Masland, 2003; Vaney, 1989).

It may be premature to relate results obtained in the rabbit to the rat as the presence of direction selective ganglion cells in the rat have yet to be established. However, direction selective GCs have been found in the retinae of other rodents such as the mouse (Yoshida et al., 2001; Weng, Sun, & He, 2005) and squirrel (Michael, 1968) and consequently may apply to the rat as well.

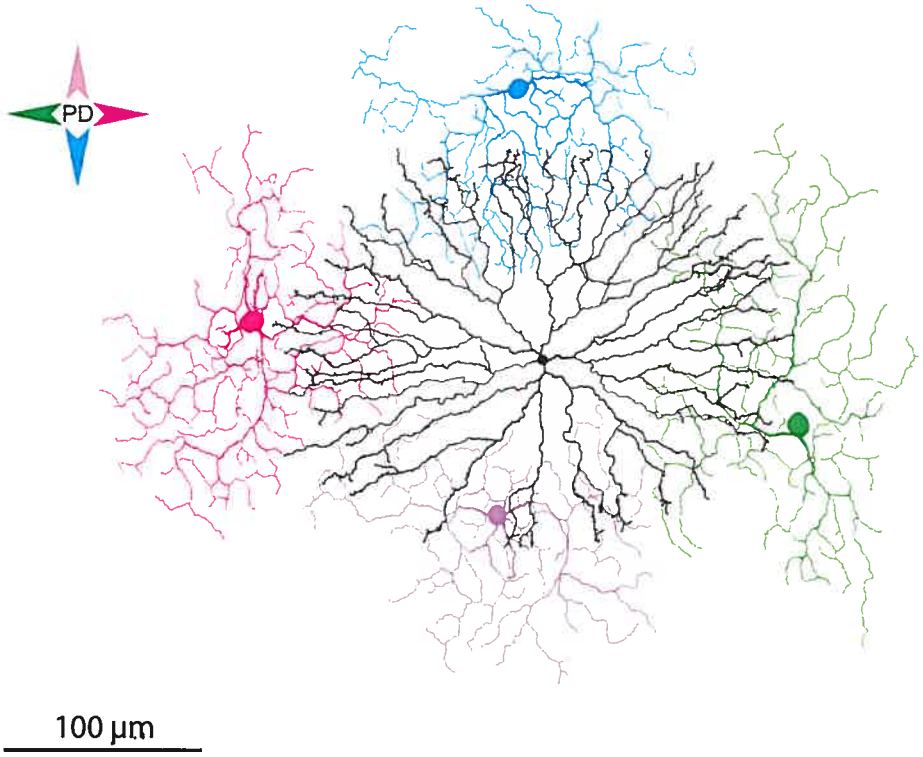

Figure 4: Selective SA cell outputs to direction selective GCs with different preferred directions. The SA cell (center - *black*) process pointing in one radial direction would selectively excite a direction selective GC (*blue, green, purple, or pink*) with the same preferred direction and selectively inhibit an overlapping direction selective GC with an opposite preferred direction.

1.4 Superior colliculus

The visual system is believed to be divided into two streams: the geniculocortical stream, responsible for the analysis of stimulus feature (i.e. form) (What pathway); and the superior colliculus, responsible for visual attention and orientation as well as multisensory integration (Where pathway) (Schneider, 1969; Rhoades & Chalupa, 1977; Rhoades, 1991).

1.4.1 Anatomical organization

The SC is a sensorimotor structure whose equivalent in lower animals (i.e. birds, reptiles) is the optic tectum. The SC appears as a large protrusion on the midbrain and is made up of alternating fibrous and cellular laminae. As with many other mammals, the rat SC consists of seven layers which are usually divided into two functional divisions. 1) The superficial layers: these include the zonal layer (Zo or layer I), the superficial gray layer (SuG or layer II), and the optic layer (Op or layer III). 2) The deep layers: consisting of the intermediate gray layer (InG or lamina IV), the intermediate white layer (InWh or lamina V), the deep gray layer (DpG or lamina VI), and the deep white layer (DpWh or layerVII) (Rhoades, 1991; Stein, 1981) (Stein and Meredith, 1991; Paxinos, 1997) (Figure 5). The occurrence of visual neurons in the SC declines with depth in the structure. Neurons of the superficial layers are almost exclusively visual, while those of the deeper laminae could fall into one of the

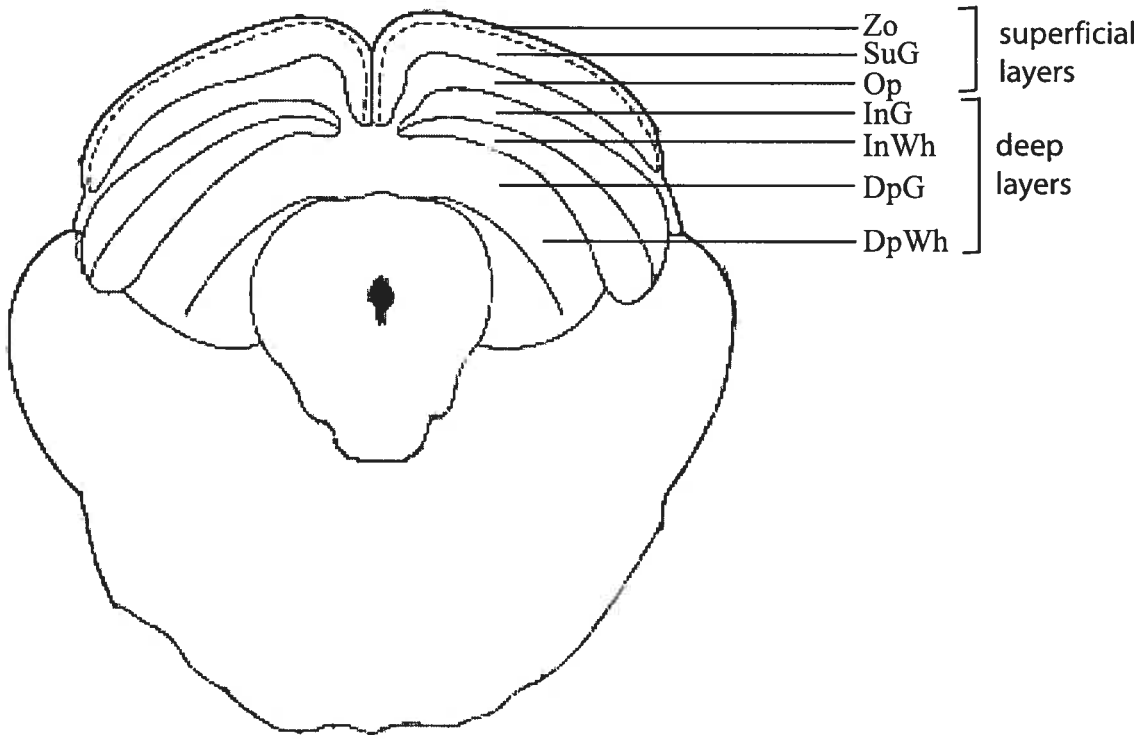

Figure 5: Location and laminar organization of the rat superior colliculus. A coronal section of the rat brain shows the laminar organization. The superficial layers of the SC include: zonal layer (Zo), the superficial gray layer (SuG), and the optic layer (Op), 2). The deep layers contain the intermediate gray layer (InG), the intermediate white layer (InWh), the deep gray layer (DpG), and the deep white layer (DpWh). *From:* Paxinos and Watson (1997).

six following categories: visual, auditory, somatosensory, motor, bimodal (ex. Visual-auditory), or multimodal (ex. Visual-auditory-somatosensory) (Rhoades et al., 1977).

1.4.2 Functional organization

In rats, the superficial layers of the SC are almost uniquely innervated by controlateral retinal inputs (Rhoades, 1991; Stein and Meredith, 1991). These inputs generate an elegant retinotopic map on the superficial layers - cells with receptive fields in nasal visual space are located rostral, whereas cells with receptive fields in temporal visual space are located caudal. Cells with receptive fields in the upper visual field are located medially and those with receptive fields in the lower visual field are located laterally. Therefore the horizontal meridian of the visual field runs rostral to caudal, and the vertical meridian runs medial to lateral (Cynader & Berman, 1972; Siminoff, Schwassmann, & Kruger, 1966). In most animals, there is also an overrepresentation of the central visual area (fovea) on the SC. This overrepresentation is more pronounced in certain animals such as cats and monkeys, and less so in others such as rodents and hamsters (Rhoades et al., 1977; Rhoades, 1991).

The occurrence of visual neurons in the SC declines with depth in the structure. Although the deeper laminae contain visual cells (Stein, 1976), this part of the structure is more involved with other sensory processes (auditory and somatosensory) and motor processes. The topographic maps for other

modalities (ie. Auditory, somatosensory, motor) are similar to those found for the visual field in the superficial layers (Stein and Meredith, 1991). This overlay of sensory maps would allow for the visual orienting of an animal towards a novel stimulus (Rhoades et al., 1977; Rhoades, 1991; Stein, 1981; Stein and Meredith, 1991).

1.4.3 Afferences of the SC

The principal afferences to the SC come from the retina and the striate and extrastriate visual cortex (Harvey & Worthington, 1990; Huerta and Harting, 1984; Rhoades, 1991; Stein and Meredith, 1991). In certain animals, for instance the rodent, the retinal inputs to the SC crossover almost completely (Lund, 1965). Over 90% of ganglion cells project toward the SC of the rat (Linden & Perry, 1983). This means that the right hemisphere of the SC contains a topographic representation of the left visual field (derived from inputs from the left eye), and the left hemisphere contains a topographic representation of the right visual field (inputs from the right eye). As this crossover of afferents is not complete, there are a few ipsilateral retinal inputs apparent (Siminoff et al., 1966; Lane, Allman, & Kaas, 1971; Diao, Wang, & Xiao, 1983). There has also been a binocular zone identified near the rostral pole of the SC (Tiao & Blakemore, 1976; Finlay, Schneps, Wilson, & Schneider, 1978; Rhoades & Chalupa, 1979; Stein & Dixon, 1979; Diao et al., 1983). The majority of direct retinal inputs terminate in the superficial layers of

the SC. There are some inputs that go directly to the deeper laminae of the SC however, most visual activity from this region is due to indirect retinal inputs such as the visual cortex. These cortical afferences to the SC are probably responsible for more complex characteristics of the receptive fields, such as binocularity (Rhoades et al., 1977; Rhoades, 1991; Stein and Meredith, 1991). There also exist projections going from one hemisphere to the other called tecto-tectal projections. There have been studies that suggest that these projections may be inhibitory in nature (Goodale, 1973; Rhoades, 1991).

1.4.4 The role of the SC in vision

The SC has been implicated in visual attention and orientation, multisensory integration, and in control of eye, pinnae and head movements towards a stimulus (Rhoades et al., 1977; Stein and Meredith, 1991). These roles of the SC are generally attributed to the deeper layers. The overwhelming majority of axons that arise within the SC exit the structure en route to the premotor and motor areas through which its sensorimotor role is expressed. Nevertheless, it is still unknown how the sensory signal in the SC is transformed into its motor input (Stein and Meredith, 1991; Rhoades, 1991). Guitton and Crommelinck (1994) proposed the foveation model in which visual information would travel dorso-ventrally, from the superficial layers to deep layers, where motor commands for ocular movement are initiated. The superficial layers are also implicated in the orientation of vision towards a novel stimulus.

Although it is generally the geniculocortical system that is attributed with the subversion of detailed analysis of stimulus features such as its form, some studies show that the SC may also play a role in this analysis via projections from the superficial layers of the SC towards the thalamus (Stein and Meredith, 1991). Also stated by Stein and Meredith (1991) is the possibility of the role of the superficial of the SC in the discrimination of visual flow and learning of new patterns (Stein and Meredith, 1991).

1.4.5 Direction selectivity in the SC

Direction selectivity is closely associated with SC neurons, not because directionally selective cells do not exist in other structures, but because a high proportion of SC neurons exhibit this property in many different species. Some examples of different species displaying this property include the cat (Berman & Cynader, 1972), mouse (Drager & Hubel, 1975), hamster (Finlay, Wilson, & Schneider, 1979; Stein et al., 1979), rat (Fukuda Y, 1978), ground squirrel (Michael, 1972), rabbit (Graham, Berman, & Murphy, 1982), and squirrel monkey (Kadoya, Wolin, & Massopust, 1971). The preferred direction varies from species to species. In the iguana (Stein & Gaither, 1981), hamster (Rhoades & Chalupa, 1976), and mouse (Drager and Hubel, 1975), the preferred direction is upward or upward and nasal. In contrast, the cat (Sterling & Wickelgren, 1969) responds best to stimuli moving nasal to temporal whereas in

the macaque monkey (Cynader et al., 1972; Goldberg & Wurtz, 1972) there seems to be no preferred direction.

Studies in the rat have shown that about 12% of visual cells demonstrate a clear direction selectivity (Fukuda, 1978; Gonzalez, Perez, Alonso, Labandeira-Garcia, & Acuna, 1992). While some researchers have noted a preference for upward direction (Fukuda, 1978), others have found no apparent tendency for a specific direction (Fortin et al., 1999).

The origin of direction selectivity in the SC is thus far unknown. It has been suggested that direction selectivity originates in the visual cortex given that cortical lesions in the cat have led to a decrease in direction selectivity in the SC. However, studies done in rats have shown that cortex activity appears after the SC displays direction selective cells (Fortin et al., 1999). In view of the fact that over 90% of retinal projections in the rat are directed to the SC, it is proposed to be the retino-collicular pathway that is important for the direction selectivity found in the SC.

1.5 The objective of this study

There were two main goals of this study. The first goal was the characterization of the anti-VAChT:saporin immunotoxin effects along rat development. Amacrine cells are the only cholinergic cells present in the retina (Chalupa & Gunhan, 2004). In order to determine the developmental course of these cells, intraocular injections of an immunotoxin (saporin-VAChT) were carried out on rats of various age groups (from date of birth to adulthood). This toxin is specific for the vesicular acetylcholine transporter and therefore eliminates all retinal cholinergic amacrine cells (Gunhan, Choudary, Landerholm, & Chalupa, 2002).

The second goal was to determine the effect of cholinergic neurons on SC cell properties, most notably direction selectivity. Electrophysiological recordings were performed to determine the influence of cholinergic amacrine cells on receptive field properties of visual neurons from the superior colliculus.

MATERIAL AND METHODS

2.1 *Experimental model*

Timed-pregnant and adult Long Evans rats were obtained from Charles Rivers Laboratories (St-Constant, Canada). The study was performed under the guidelines established by the Canadian Council for the Protection of Animals regarding the care and use of animals for experimental procedures. The study involved 92 rats, male and female, of various ages (Table I and II). Of the 92 rats, 22 were normal (i.e. did not receive any intravitreal injections), 26 were controls and received intravitreal vehicle injections (i.e. saline-injected), and 44 were treated and received intravitreal immunotoxin injections (i.e. toxin-injected). The amount of fluid injected depended on the age of the rat. The two injected groups received injections at various ages and were raised to adulthood before any immunohistochemistry was performed. This was done to determine how the immunotoxin affected SA cells during different stages of their development. All 3 groups had subjects (normal, n = 22; saline, n = 10; toxin, n = 5) that had electrophysiological recordings done at the level of the SC. All recordings were done once the animal reached adulthood.

2.2 *Preparation of animal for intravitreal injection*

Since the effect of the novel immunotoxin against the vesicular acetylcholine transporter (anti-VAChT) (immunotoxin was already diluted in sterile saline) was to be tested on various postnatally aged rats, the anaesthesia

	Age at injection	*No. of subjects*	*Volume injected(µl)*	*Age at sacrifice*	*Protocol applied*
Saline-injected	P4	8	3	> P60	histology
Toxin-injected	P4	10-1*	3	> P60	histology

Table I: The group of subjects that were submitted to intravitreal injections using the 'old' protocol. The protocol used in this group was that used by Gunhan and colleagues (Gunhan et al, 2002). These subjects had no electrophysiological recordings done; only immunohistochemistry was performed on the retinas.

** One subject died during the surgical procedure.*

Table II: The group of subjects that were submitted to intravitreal injections using the 'new' protocol. The protocol used in this group was developed by the laboratory of Dr. Casanova. Certain subjects had both electrophysiological recordings done in the SC and immunohistochemistry of the retinas. ** Two subjects died during the surgical procedure.*

	Age at injection	*No. of subjects*	*Volume injected(μl)*	*Age at sacrifice*	*Protocol applied*
Saline-injected	P1	18	1.5-2	> P60	histology and electrophysiology
Toxin-injected	P1	6	1.5	P8	histology
		6	1.5	> P60	
	P4	10	1.5-2	> P60	histology and electrophysiology
	P2	2	1.5	P9	histology
		2	1.5	P16	histology
	P6	2	2	P13	histology
		2	2	P20	histology
	P12	2-1*	2	P19	histology
		2-1*	2	P26	histology
	P60	1	3	P67	histology
		1	3	P74	histology
		2	5	P74	histology

protocol employed varied with the age of the animal. All pups were handled in sterile conditions since they would be replaced with the mother. Therefore, pups were taken from the mother using sterile gloves and placed in a sterile surgical mask for transportation to the incubator where they were placed on a disposable underpad. One rat pup at a time was placed directly onto and covered with crushed ice to prevent the pup from moving – air pockets were present so the animal could breath. Hypothermia was achieved in 8-10 minutes for each pup. Rats older than P2 were anesthetized with isoflurane 4-5% for 5-7 minutes and then isoflurane was reduced to 2%. Animals remained anesthetized for the duration of the surgical procedure (approximately 3 minutes). Once the surgical procedure was completed, pups were re-placed in the incubator until fully awake and normal body temperature was achieved, then transferred along with their mother using sterile gloves. Adult rats were put back in their cage where they once again became fully active. Excluding anesthesia protocols, all aspects of surgery were the same for all groups.

The anesthetized animal was placed under an operating microscope in order to perform the surgery. If the animal was less than post-natal day 14 (P14), an incision of the eyelid needed to be performed because the eyelid was still closed at this point; this was done using an ophthalmic scalpel (Micro Feather). As this was the first study to attempt intravitreal injections in rats at P0, it was necessary to devise a novel protocol in order to perform injections in eyes of such small size. Our first protocol was developed by the laboratory of Dr. Chalupa (Gunhan et al, 2002) (i.e. *'old'* protocol). A scleral pilot hole at the

most posterior region of the eye was made using a 30 gauge needle in order to facilitate penetration of the underlying sclera, choroids, and retina by a blunt-tip needle which is connected to a 10μl glass syringe (Hamilton, Reno, NV) by polyethylene tubing prefilled with distilled water prior to drawing up the fluid (vehicle or immunotoxin). An air bubble was created between the distilled water and the material being injected. The vehicle or immunotoxin was injected into the vitreous chamber where the pilot hole had already been made. This route of administration avoided injury to other structures of the eye such as the iris or lens. The volume of fluid injected into the animals eye varied being that the size of the eye was dependant on the animals age (Table III). The injection was performed at an oblique angle to the eye and was given slowly over 1 to 2 minutes to allow for diffusion of the fluid. After each injection, the eyelid was resealed (if it had been surgically opened) using a tissue adhesive (VetBond^{TM}, 3M) and an ophthalmic ointment (Neomycin and Polymyxin B Sulfates and Bactracin Zinc, Bausch & Lomb®) was applied to prevent any infection. This protocol proved to be inaccurate since it did not inject the required amount with each injection. Therefore, a second intravitreal injection protocol was developed in our laboratory during the course of this study. A scleral pilot hole was made using a 31 gauge needle to ease penetration by a tapered glass micropipette (inner diameter of 1.5mm) with a tip diameter of 25 to 30µm and a tip length of

Age at Injection	*Volume injected (µl)*
P0-P2	1.5-2
P6	2
P12	2
P21	3
>P60	5

Table III: Volume of an intravitreal injection varied with age of rat. The volume of an intravitreal injection depended on the age of the rat since the size of the eye increased with age.

2.5mm (Figure 6). It was found that glass micropipettes were preferable to metal needles because the tip diameter was smaller, the depth of injection was easier to standardize, and the tapered pipette tip effectively seals the injection site during injection, therefore reducing leakage of the injected fluid from the eye. The tapered micropipette was connected to a 10 μl glass syringe (Hamilton, Reno, NV) by a 15cm long polyethylene tubing (Portex FiniBore, UK; outer diameter of 0.8mm and inner diameter of 0.4mm) pre-filled with heavy mineral oil (Rougier®) prior to drawing up the fluid (saline or immunotoxin). All junctions on this apparatus were sealed with epoxy ricin. Injections were performed in the same manner as in the first protocol.

2.3 Testing of anaesthesia protocols

We tested two different anaesthetics to determine which would be best in order to perform electrophysiological recordings in adult rats at the level of the SC. We tested both ketamine and urethane. Ketamine 80mg/kg (Wyeth-Ayerst Canada, Inc.) was injected intraperiteonally in 3 adult rats. Levels of anaesthesia were determined by response to hindpaw pinch every half hour and maintenance doses of 80 mg/kg (intra-muscular) were given when required.

Another group of rats received an intraperitoneal (IP) injection of urethane (Sigma®) 1250 – 1500 mg/kg at different concentrations (15%, 20%, 25%, 30%, 40%, 50%, 60%, 70%, and 80%). The same protocol for monitoring

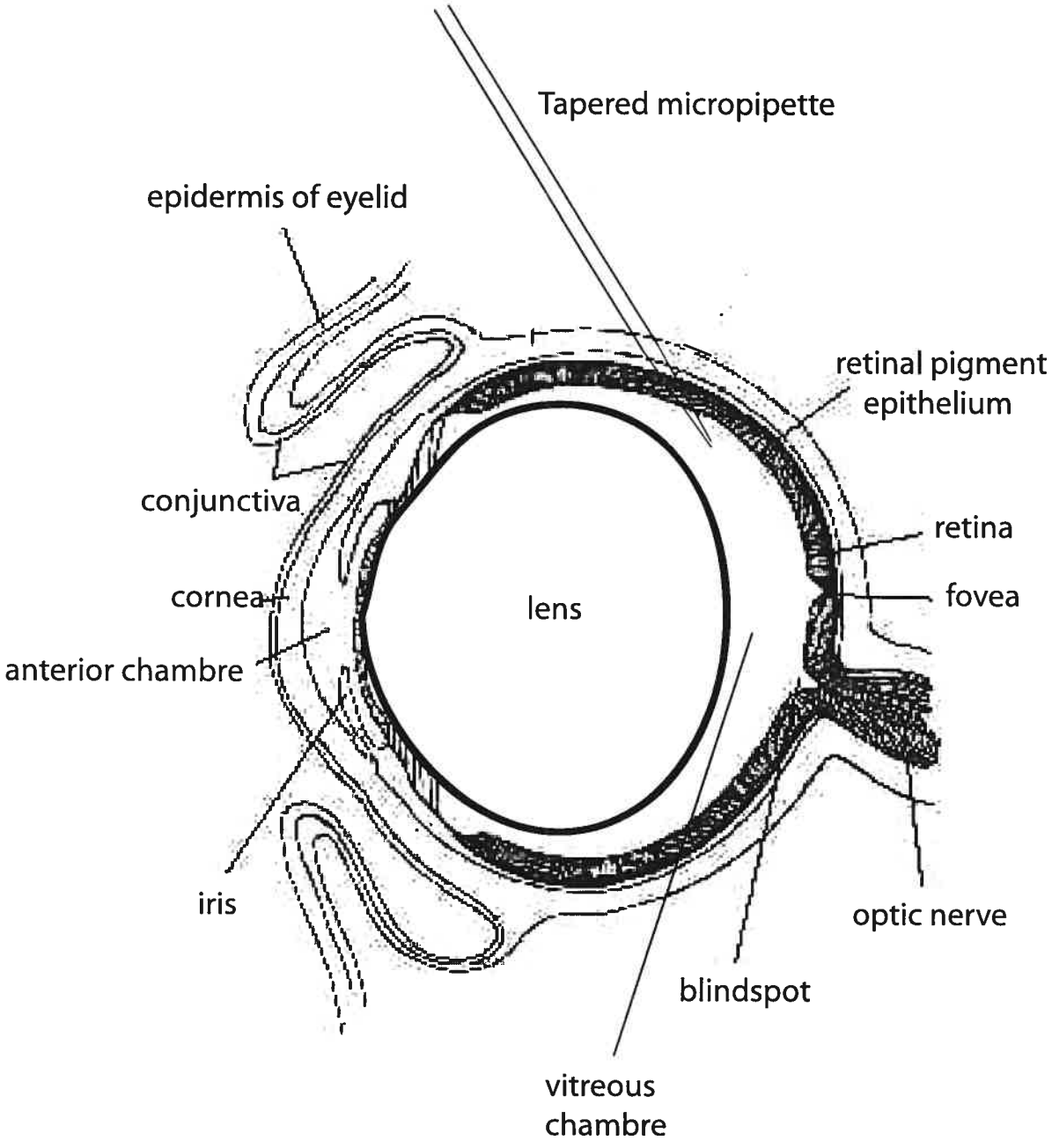

Figure 5: Schematic representation of an intravitreal injection in the rat eye. The injection is performed at an oblique angle through the dorsal hemisphere of the eye and micropipette was inserted through the sclera to a standardized depth, so as to avoid injury to the lens.

Modified from: http://www.ratbehavior.org/Eyes.htm

anaesthesia levels used for ketamine experiments were employed here. Maintenance doses consisted of 0.1 – 0.2ml of urethane 1500mg/kg.

2.4 Preparation of animal for electrophysiological recordings

The adult animals were anesthetized with an intraperitoneal injection of urethane 30% (1.25-1.5g/kg) (Sigma®). A rectal probe and a heating pad placed under the animal were used to ensure a constant body temperature of 37-37.5°C. Hindpaw reflex and electrocardiogram (ECG) were regularly monitored in order to maintain a proper level of anesthesia. Pupils were dilated with the use of ophthalmic drops of atropine sulfate 1% (Isopto® Atropine). The corneas were kept moist by periodically applying carboxymethylcellulose (Celluvisc®, Allergan).

The animals were placed on a stereotaxic frame. Craniotomies were performed over the contralateral hemisphere of the eye being tested (immunotoxin-injected; saline-injected; untreated). Coordinates for the SC were anywhere between –5 to –8mm Bregma and 0.5 to 3 medio-lateral (co-ordinates from Paxinos and Watson, 1997). The dura mater was then excised and electrodes were lowered into the SC. The cortex was constantly irrigated with artificial cerebrospinal fluid (aCSF) throughout the surgical procedure. Finally, the cortex was covered with agar 2% to prevent drying out of the cortex.

2.5 *Single-unit extracellular recordings*

Extracellular recordings of single cells in the superior colliculus were done using tungsten microelectrodes (A&M Systems, inc©., Carlborg, Washington State, USA) of an impedance between 1 and 5MΩ. The cellular response was then amplified with the aid of an amplifier (Grass®, Astro-Med Inc.) and transmitted to an oscilloscope (Kikusui®) and audio monitor. The cellular signal passes through HumBug® (Quest Scientific) – a system that eliminated electrical signals from analog signals. Action potentials were isolated from the spontaneous activity using a window discriminator (WPI). The signal was then fed to the acquisition program (Spike2.15, CED Cambridge, UK) via an analog digital interface (1401, CED). The responses were recorded as post-stimulus time histograms (PSTH) of 10 ms bin width.

2.6 *Visual stimulation*

The animal was placed parallel to a translucide screen 28.5cm away from the eye being stimulated. Once a visual response was found, the receptive field was first mapped and its limits were established using a manually controlled stimulus projected onto a screen parallel to the animals eye using a hand-held projector and an ophthalmoscope. Quantitative testing of each visual cell was then carried out using stimulation generation software, VPixx (Sentinel Medical Research Corp., Quebec, Canada) run by a MacIntosh computer. The

stimuli were back projected by a LCD projector (NEC) onto the translucide screen parallel to the animal covering 80° x 107° of the visual angle. If the receptive field for a given visual unit was found and mapped, the stimuli were presented within the limits of its receptive field. Otherwise, full-screen stimuli were presented to the visual cell. Once receptive field properties were characterized, we proceeded to quantitatively analyze the cell's properties (spatial frequency, temporal frequency, contrast, preferred direction/orientation) using sinusoidal drifting gratings. In order to determine the spontaneous activity level of a cell, the activity for a blank screen of equal mean luminance was quantified during each test. Each stimulus presentation lasted for 4 seconds and was repeated 4 times. Presentations were randomly interleaved and only the tested eye was exposed to the stimulus.

2.7 Receptive field properties studied

The main property of interest for an individual neuron was its preferred direction. Each cell's properties (spatial and temporal frequency and contrast) were first optimized in order to determine the preferred direction/orientation.

2.7.1 Direction selectivity

To determine the direction selectivity of a visual neuron, a drifting sinusoidal grating was presented to the animal at various orientations (between 0° and 360°, intervals of 15° or 30°). The orientation curve reflects the mean response of a cell (action potentials/second) to each of the orientations presented. The bandwidth represents the degree of selectivity of the cell for orientation; it is represented in degrees and corresponds to the mid-width of the curve measured at the mid-height of the curve. The orientation curve also contains information relative to the direction selectivity of movement of the tested cell. Although gratings presented at, for example, 0° and 180°, are oriented in the same sense, they move in opposite directions. In order to quantify this property, a direction selectivity index (DI) is calculated with the following formula:

$$DI = 1 - \frac{\textit{response amplitude for the non-preferred direction} - \textit{spontaneous activity}}{\textit{response amplitude for the preferred direction} - \textit{spontaneous activity}}$$

The non-preferred direction is represented by the direction 180° $\pm$ 30° away from the preferred direction. A neuron with a DI > 0.5 is considered to be

selective for direction, and a cell with a DI < 0.5 is said to be non-selective for direction (Casanova et al, 1992).

2.7.2 Spatial frequency

The spatial frequency (SF) is the number of cycles per degree. To determine the preferred SF of the cell, various SFs are presented at the cell's preferred direction. This test allows for the discovery of the preferred SF as well as the spatial resolution of the cell. That is to say, the maximum frequency the cell is able to respond to, as well as the minimum frequency that will elicit a cellular response. The SF curve indicates the preferred SF and also the level of selectivity for this preference. The bandwidth is expressed in octaves and corresponds to the full-width of the curve measured at the mid-height of the curve. A cell can have one of three types of responses which is represented by the shape of its response curve; (1) bandpass (a Gaussian curve), where a cell has an optimal SF; (2) low-pass, where a cell responds with no attenuation to low SFs; and (3) high-pass, where a cell responds with no attenuation to high SFs.

2.7.3 Temporal frequency

Temporal frequency (TF) represents the number of cycles per second (Hz). To determine the preferred TF of a cell, we present a grating optimized for

orientation/direction and spatial frequency at different TFs. The same methods employed for spatial frequency were used in this instance to determine the optimal TF, degree of selectivity and temporal resolution.

2.7.4 Velocity

When the optimal spatial and temporal frequencies were available for a cell, we were able to determine the preferred velocity of the cell. The velocity of a stimulus was calculated by the following equation:

$$\text{Velocity} = \frac{\textit{Spatial frequency (c/°)}}{\textit{Temporal frequency (c/s)}}$$

2.7.5 Contrast sensitivity

In order to determine the contrast sensitivity of a cell, the contrast level of the stimuli was varied from 0 to 100% contrast and presented to the animal. Under each stimulus condition, the action potentials of the cell were collected for each repetition, averaged and normalized, where the maximal response for each cell was taken as 100%. The shape of the curve obtained allows for the determination of the C50 (50% of the maximum response), contrast threshold, and function – sigmoidal, log or linear.

2.8 Verification of neuroanatomical sites of recordings in the SC

To prove all recordings were done in the SC, electrolytic lesions were performed along the electrode penetration. Using a lesion maker, a current of 5μA was passed through the electrode for four seconds, at three different locations of penetration (moving from the most ventral to dorsal position). The animal was euthanized at the end of the experiment using an overdose of either halothane or isoflurane (via inhalation). The electrocardiogram (ECG) was used to confirm the death of the animal. The animal was then subject to an injection of heparin directly into the left ventricle of the heart. Following intracardial perfusion of the animal using phosphate-buffer saline (PBS) 0.1M at pH 7.3 and paraformaldehyde (PFA) 4%, the brain was removed and placed in PFA 4% for 24 hours. The brain was then transferred to a sucrose solution 10% (12 hours), then 20% (12 hours), and finally 30% (12 hours). Finally, the brain was cut in coronal sections of 40μm thickness with the aid of a microtome (Leica). Half the sections were treated with violet cresyl, the other half with a solution that reveals the enzyme acetylcholinesterase (AChE). The SGS of the SC is an AChE-rich layer, and therefore, has a darker appearance once treated with this solution (Paxinos and Watson, 1986).

2.9 Revelation of cholinergic neurons of the retina

Animals were euthanized with an overdose of halothane or isoflurane (via inhalation) at ages ranging from P6 to adult, and then perfused with PBS and PFA 4%. The dorsal part of the eye was marked so as to keep note of the orientation of the eye, and the eyecups were then removed. An incision was made at the outer limit of the cornea using an ophthalmic scalpel (Micro Feather), and microscissors were then employed so the cornea could be removed. A PBS solution was used throughout the procedure to keep the eye well hydrated. A notch was made at the marking indicating the dorsal part of the eye. The eye was post-fixed in PFA 4% for 30 minutes; once removed from the PFA 4% solution, the eye was rinsed with PBS solution. The lens was finally excised and the eye placed in a sucrose solution 30% overnight to cyroprotect the tissue.

All retinal samples were processed for post embedding immunohistochemistry according to the methods established by Gunhan et al (2002). The eyes were placed in frozen tissue embedding matrix (HistoPrep, Fisher Scientific). A microtome was used to cut cross-sections of 20μm, which were then mounted on gelatine-coated slides. Cross-sections of the treated eye and the contralateral control eye were placed on the same slide so that both eyes would receive the same treatment. The slides were then placed in an incubator at 37°C for 2 hours; this ensured that the cross-sections would stay mounted on the slides during the course of the immunohistochemistry. The slides were then

pre-incubated with a PBS solution containing normal donkey serum (NDS) 10%, (BSA) 2.5%, 0.5% Triton X-100 for 2 hours. These were then put through a wash cycle, which involved rinsing with a mixture of 0.3% Triton X-100 in PBS, followed by three washes in PBS. Goat anti-choline acetyltransferase (ChAT) affinity purified polyclonal antibody (Chemicon International, Temecula, CA), the primary antibody, was diluted (1:50) in a blocking solution containing (NDS) 10%, (BSA) 2.5%, triton-X 0.5% and cross-sections were incubated with this solution overnight at 4%. The next day, these sections were put through the wash cycle, and then incubated with a fluorescent secondary antibody, fluorescein (FITC)-conjugated AffiniPure donkey anti-goat IgG (Jackson ImmunoResearch Laboratories, Inc., Mississauga, ON), diluted 1:600 PBS-BSA for 1 hour at room temperature. After a final cycle, slides were coverslipped with Vectashield mounting media (Vector Laboratories). Fluorescence marked any retinal cholinergic neurons present and images of the retinal slides were taken using a Leica (DMR) binocular microscope equipped with a CCD camera (Retiga) 1300, QImaging.

RESULTS

3.1 Introductory remarks

Preliminary results of this study showed that two techniques employed in this project had to be ameliorated before this study could be fully commenced. Firstly, we had difficulties with anaesthesia of adult rats for electrophysiological recordings. Secondly, immunohistological results demonstrated that there was no elimination of cholinergic cells in the retina following intravitreal injections of anti-VAChT:saporin immunotoxin. The first technique to be addressed was the anaesthesia protocol employed for the electrophysiological study; the second was the intravitreal injection protocol utilized for rat pups.

Once the technical problems were rectified we performed electrophysiological recordings in the SC of normal and treated adult animals. Later histological analysis of the retina of treated animals showed that a large majority of cholinergic neurons were still present when it was expected that these cells would be completely eliminated. This then led to our focus on the developmental course of cholinergic SA cells in the retina and how they were affected by the anti-VAChT:saporin immunotoxin.

3.2 Technical improvements in material and methods

3.2.1 Anaesthesia

Different anaesthesia protocols were tested on adult rats to determine which would be the most reliable to employ during electrophysiological recordings in the SC. We attempted to anaesthetize adult rats with two different kinds of anaesthetics. Both had previously been used in rat electrophysiological studies in the SC. The first experiment using ketamine 80mg/kg intraperiteonally was not successful in keeping the rat anaesthetized for periods longer than an hour without giving the animal a maintenance dose at the end of each hour. As experiments could last up to 10 hours or more, we found this anaesthetic required the animal to be injected too frequently during the course of the experiment (ranging from 10-12 times, depending on the length of the experiment). The other anaesthetic we tested was urethane 1250 – 1500mg/kg intraperiteonally. Here, we found that high concentrations levels (40 – 80%) caused the animal to die within 2 - 4 hours after the initial injection, while low concentrations (15 - 25%) required large amounts of solution to be injected intraperiteonally. Finally, urethane 30% IP was considered the best anaesthetic to use in our rats as it allowed animals to achieve anaesthesia rather quickly (10-30 minutes) and maintenance doses (0.1 – 0.2 ml) were required only every 6 to 7 hours.

3.2.2 Intravitreal injections

Initial intravitreal injections in this study were performed using the 'old' protocol supplied by Dr. L. Chalupa's laboratory of University of California at Davis. Results from this study demonstrated that there was no elimination of cholinergic neurons. During the surgical procedure, we noticed that the amount of immunotoxin reaching the eye was not standardized and there was extensive leakage once the injection was performed. This led us to develop a 'new' protocol for intravitreal injections. The new protocol was able to inject a precise amount of the immunotoxin and produced no or very little leakage once the procedure was completed (see Material and Methods section for a detailed description of both protocols).

3.3 Effect of VAChT-saporin immunotoxin using the new injection protocol

Since the old protocol was ineffective, we developed a new protocol for intravitreal injections (see Material and Methods section) and the following results were obtained with this improved procedure.

Six rats received intravitreal injections of the VAChT-saporin immunotoxin at P1. Animals were euthanized one week later and retinae processed to determine if the injections were successful. Figure 7 shows the non-treated and immunotoxin-treated retinae from the same rat. The ChAT immunoreactivity was clearly evident in both central and peripheral regions of the non-treated retina (Figure 7A). ChAT labeling was most notable within the

Figure 7: Cholinergic amacrine cells in the developing rat retina. The images are vertical sections of P8 retinae from a rat treated at P1. **A)** In central and peripheral regions of the normal retina, there is heavy labelling of cell bodies in the GCL and INL. Also seen are the clearly labelled dendritic arborizations in the IPL. **B)** Almost complete elimination of immunoreactivity is noted in the treated eye. There is some weak labelling of cell bodies still present. GCL: ganglion cell layer; INL: inner nuclear layer; IPL: inner plexiform layer.

A

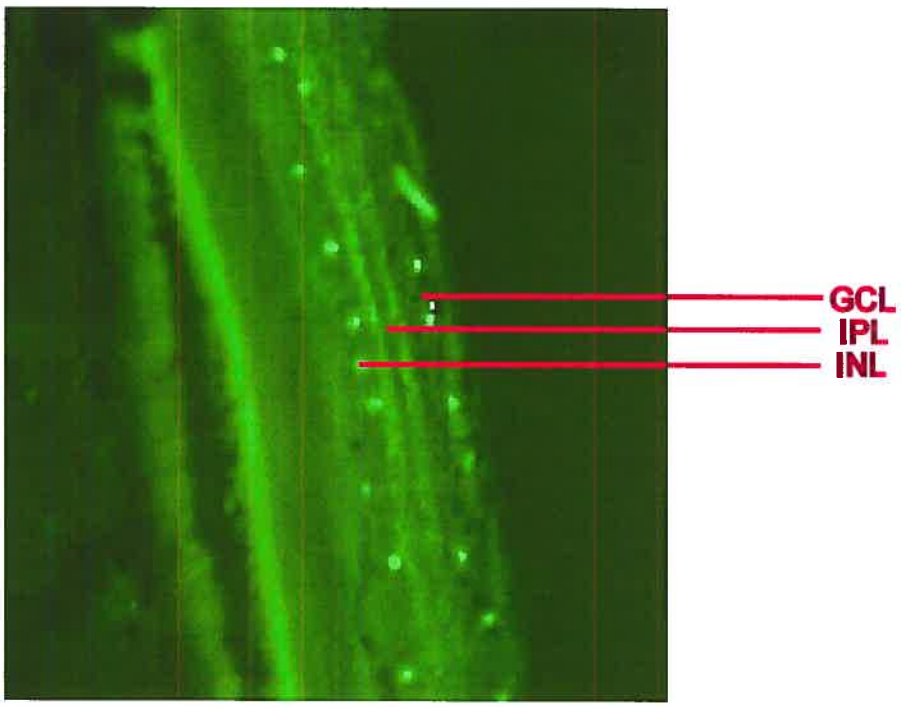

03M1706

B

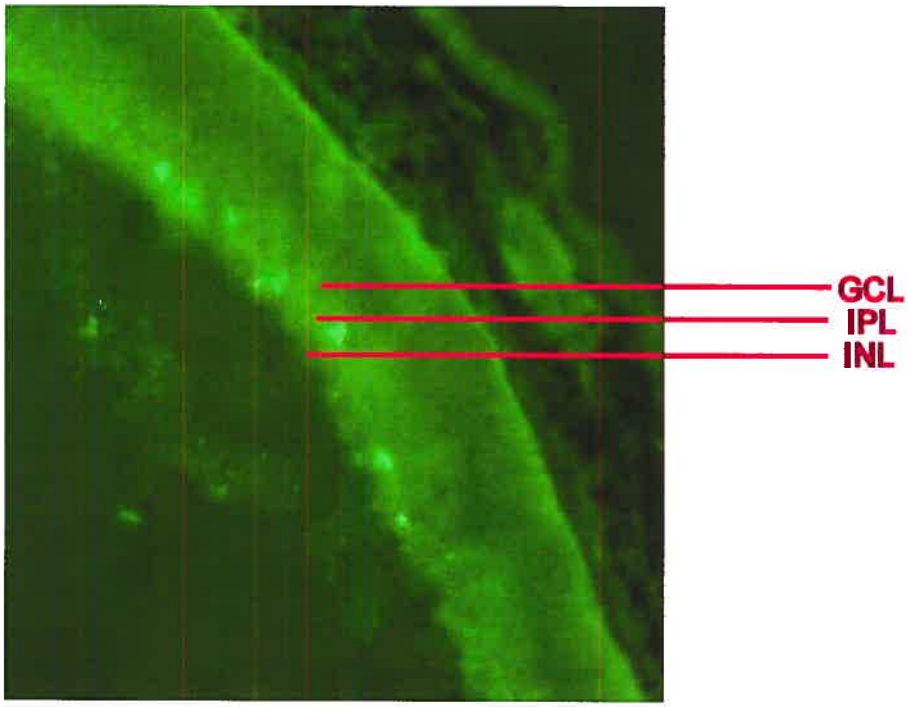

03M1706

0.1 mm

IPL as two distinct strata of cholinergic processes. Also noted was the labelling of the soma of cholinergic neurons. In contrast, the immunotoxin-treated retina (Figure 7B) showed a marked decrease in ChAT immunoreactivity with only a few cell bodies labelled. The toxin had an effect on 5 out of the 6 subjects.

3.4 Impact of retinal cholinergic cells on activity in the SC

From the immunohistochemical results of the prior experiment, it was concluded that the VAChT-saporin immunotoxin was able to eliminate the majority of cholinergic amacrine neurons from the retina. Therefore, intravitreal injections of the toxin were then performed in newborn rats. The animals were raised to adulthood at which point electrophysiological recordings could be performed. This was done so as to determine if the lack of SA cells would affect the receptive field properties of visual cells in the SC. Recordings were done in 27 adult rats. Of these, 22 were normal subjects and 5 were treated subjects who had an intravitreal injection done at P2. All saline-injected rats died during electrophysiological recording sessions and did not produce any results.

3.4.1 Physiological properties of visual SC neurons in normal rats

3.4.1.1 Direction selectivity

A total of 32 visual cells were tested quantitatively for direction selectivity in normal subjects; 26 cells were found to be 'orientation' selective and 6 cells were not selective for any orientation. Of these, only 19.2 % were

direction selective cells (DI > 0.5). The distribution of DIs is presented in figure 8A; the mean direction index was 0.34 $\pm$ 0.24. In most direction selective neurons, the preferred direction was very broadly tuned. Figure 8B illustrates the bandwidth distribution in our population, showing most cells as being broadly tuned (mean bandwidth = 48.5 $\pm$ 24). Depicted in figure 9 is a typical direction selective cell (A) and 'orientation' selective cell (B) encountered in a normal subject. The 'orientation' selective cell refers to a cell that responded selectively to motion on one axis (ex. 0° and 180°). The direction selective cell responded optimally to gratings with an orientation of 45°, but was broadly tuned and had a bandwidth of 96.4° with a DI = 0.74. The 'orientation' selective cell was tuned broadly to gratings with an optimal orientation of 270°. It responded slightly more weakly to gratings of the same orientation but moving in the opposite direction (90°). The DI for this cell was 0.17.

3.4.1.2 Spatial frequency

27 visual cells were tested for spatial frequency in normal rats and we found that, generally, visual neurons of the SC responded optimally to stimuli with a low spatial frequency (< 0.07 c/deg). The mean spatial frequency was 0.03 c/°. Among the neurons from the normal group tested for SF, 14 had a low pass response profile and 13 were broadly tuned for low frequencies. Figure 10 shows examples of typical response curves for SF found in our population. Panel A represents a unit with a low pass response profile to increasing SF. Panel B shows a bandpass cell with a preferred SF of 0.05 c/°. The mean bandwidth of cells with bandpass spatial frequency tuning was 2.73 $\pm$ 1.3

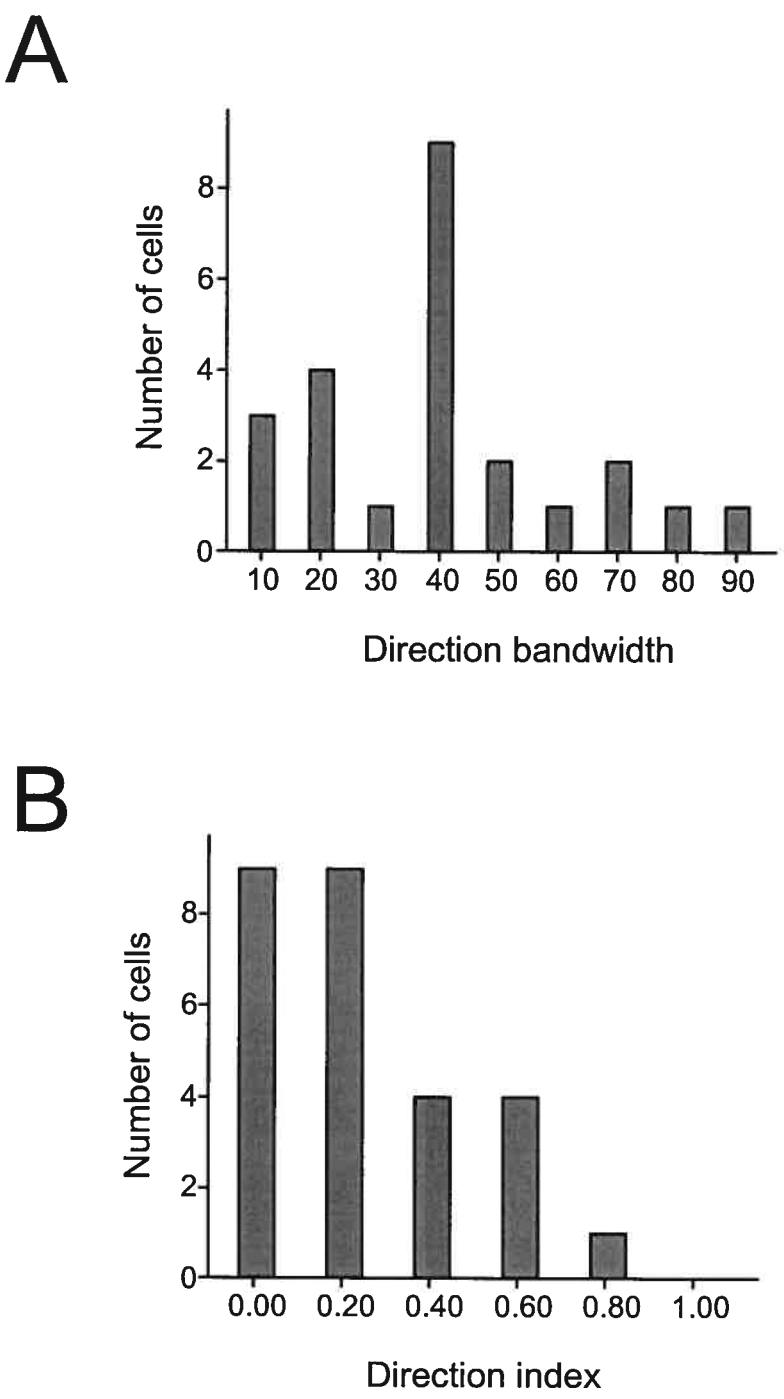

Figure 8: Distribution of DIs and bandwidths for normal animals. **A)** Distribution of DIs in the normal subjects, where the mean DI is $0.34 \pm 0.24°$. **B)** The broad direction tuned function is represented here by the bandwidth distribution where a high proportion of cells display a bandwidth of $48.5 \pm 24°$.

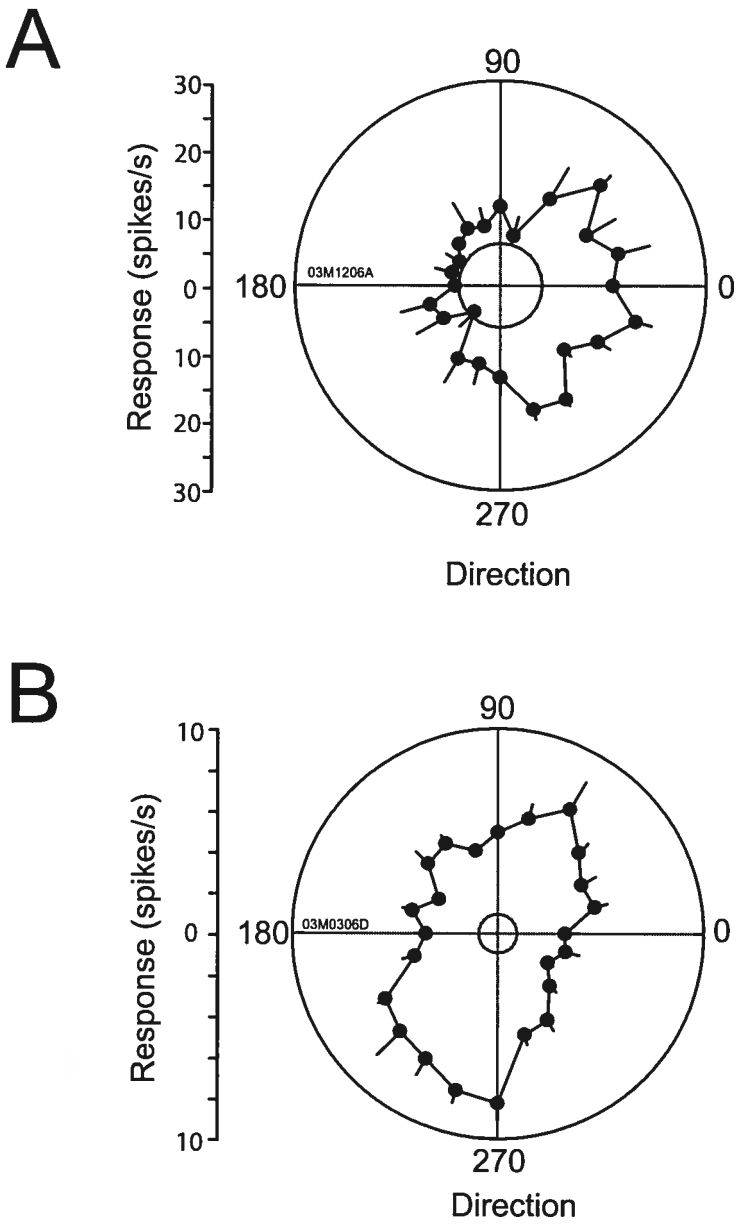

Figure 9: Example of a direction and 'orientation' selective neuron from normal subjects. **A)** Response of a broadly tuned direction selective cell for 45°. **B)** A typical 'orientation' selective cell found in the normal group; this neuron is selective for a direction of 270° and almost equally selective for the grating moving in the opposite direction (90°). Responses are shown as mean ± S.E.M and are represented by solid lines. Dotted lines represent spontaneous activity levels.

Figure 10: Response of SC cells from normal rats to the spatial frequency of drifting gratings. **A)** Spatial frequency tuning for a cell with a lowpass response profile. **B)** An example of a bandpass cell tuned for a spatial frequency (0.05 c/°). Responses are shown as mean ± S.E.M and are represented by solid lines. Dotted lines represent spontaneous activity levels. **C)** Distribution of optimal spatial frequencies show cells respond to SFs ranging from 0.005 to 0.09 c/° with a mean optimal SF of 0.026c/°.

A

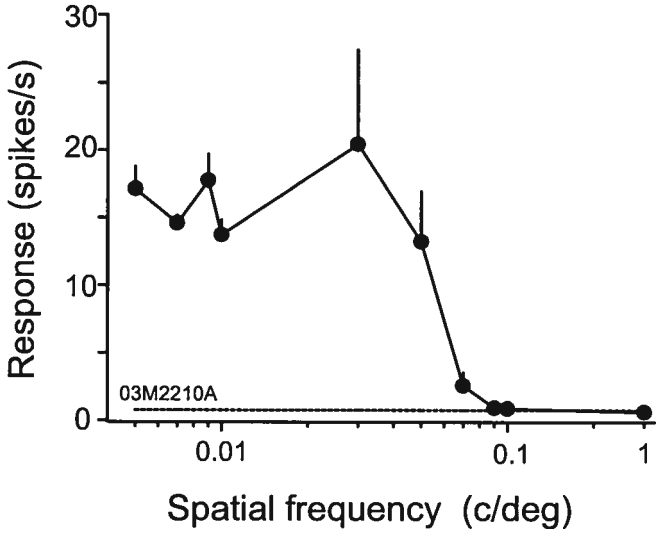
30
20
10
0
Response (spikes/s)
03M2210A
0.01
0.1
1
Spatial frequency (c/deg)

B

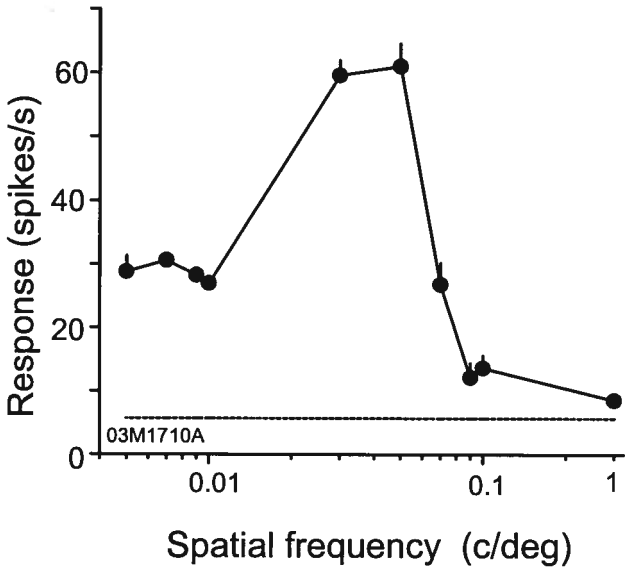
60
40
20
0
Response (spikes/s)
03M1710A
0.01
0.1
1
Spatial frequency (c/deg)

C

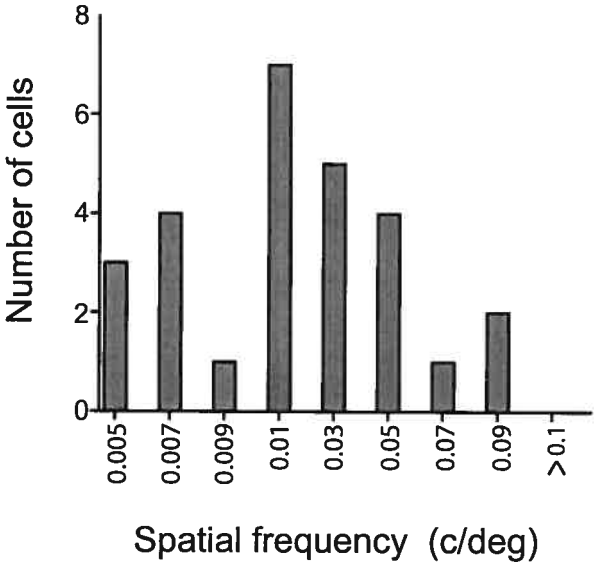
8
6
4
2
0
Number of cells
0.005
0.007
0.009
0.01
0.03
0.05
0.07
0.09
>0.1
Spatial frequency (c/deg)

octaves. The distribution of optimal spatial frequencies is represented in figure 10C. The optimal SFs for normal animals ranged from 0.005 to 0.09 c/deg, with a mean optimal SF of 0.026c/deg. This graph also points out that most cells preferred a SF of 0.01 c/°.

3.4.1.3 Temporal frequency

A total of 28 visual neurons from normal subjects were tested for temporal frequency. Of the 28 cells, 10 were not selective for any temporal frequency, 14 were clearly selective for a particular frequency, and 4 had a low pass response profile. The mean optimal temporal frequency was 2.3 $\pm$ 0.99 c/sec, and the mean bandwidth was 2.2 $\pm$ 0.71 octaves. Representative examples of a SC cell response, as a function of temporal frequency, are presented in figure 11A and B. Panel C shows the distribution of optimal temporal frequencies for the normal group, where there is a clear preference for a TF of 2 c/sec within the group of cells selective for TF.

3.4.1.4 Contrast sensitivity

23 cells were tested for the effect of contrast on the response of visual cells of the SC. An increase in cell response along with stimulus contrast (ranging from 0 to 100%) was observed with a mean optimal contrast level of 85.5 $\pm$ 12.3%. Figure 12 shows the normalized responses of 3 cells expressed as the percentage of the maximal response, plotted against the stimulus contrast. Response curves were either sigmoidal (n = 4), log (n = 10) or linear (n = 9) in

Figure 11: Temporal frequency tuning and distribution of optimal TFs. **A)** Example of a neuron with a lowpass response profile **B)** Illustration of a bandpass cell tuned for 2 Hz. Responses are shown as mean ± S.E.M and are represented by solid lines. Dotted lines represent spontaneous activity levels. **C)** The distribution profile for optimal TFs. The mean optimal TF is 2.3 $\pm$ 0.99 c/sec. NP: no preference for a TF.

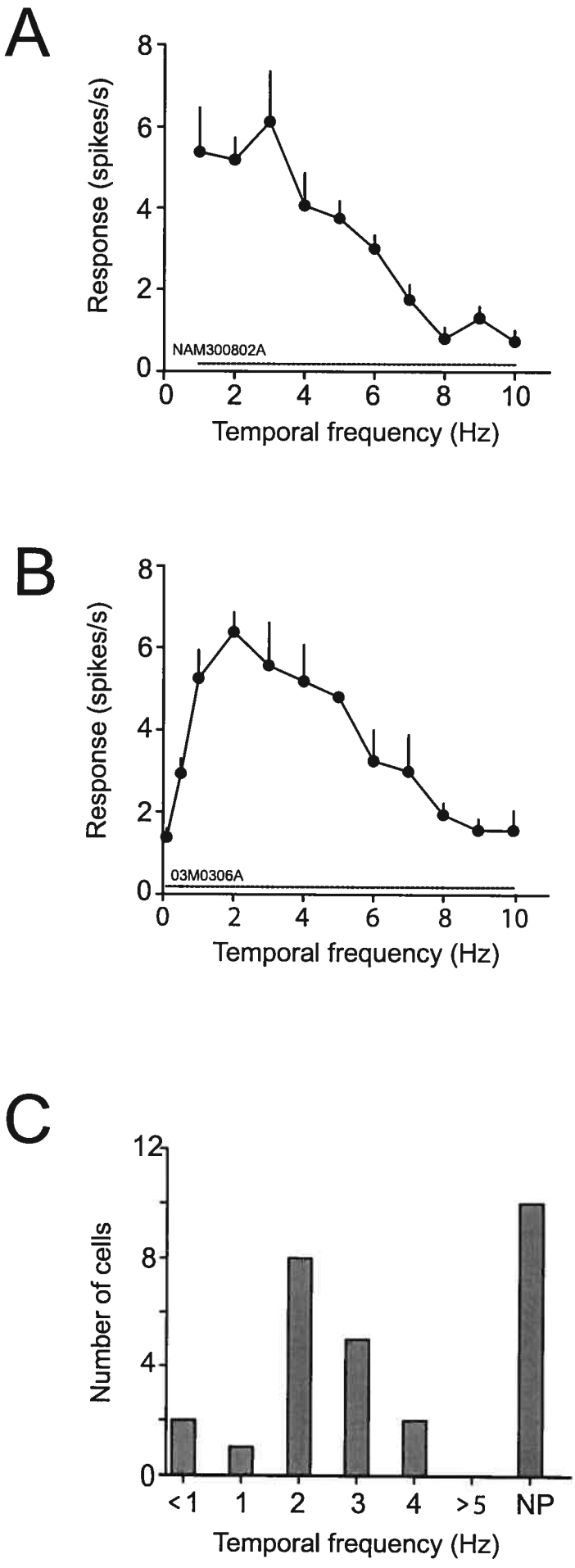
A
Response (spikes/s)
NAM300802A
Temporal frequency (Hz)
B
Response (spikes/s)
03M0306A
Temporal frequency (Hz)
C
Number of cells
<1
1
2
3
4
>5
NP
Temporal frequency (Hz)

Figure 12: Response of a cell as a function of stimulus contrast. Of the 23 cells tested for contrast, 17.5% had a sigmoidal response curve **(A)**, 43.4% had a log response curve **(B)**, and 39.1% had a linear curve **(C)**. All responses have been normalized as the percentage of the maximal response.

A

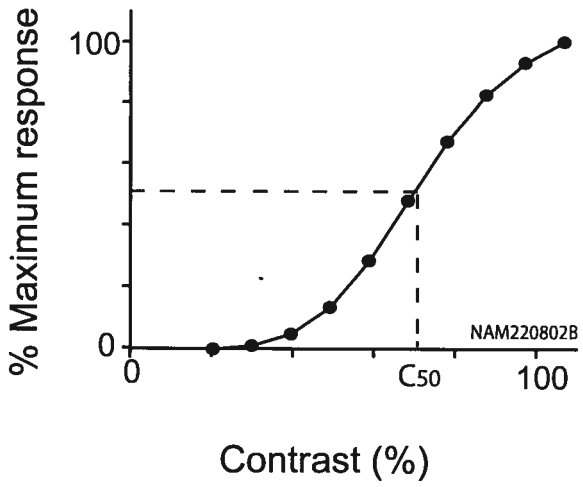
% Maximum response
100
0
0
C50
100
NAM220802B
Contrast (%)

B

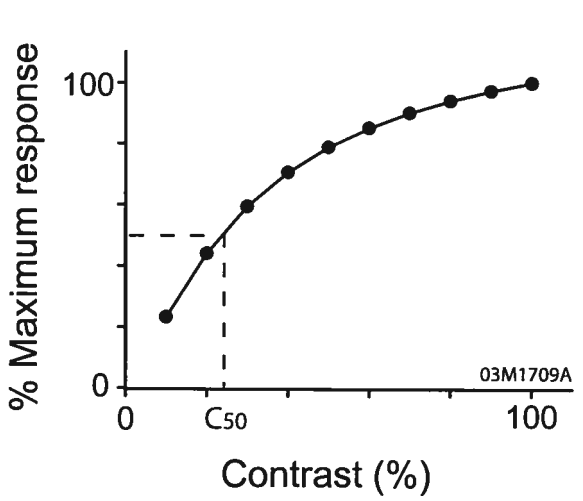
% Maximum response
100
0
0
C50
100
03M1709A
Contrast (%)

C

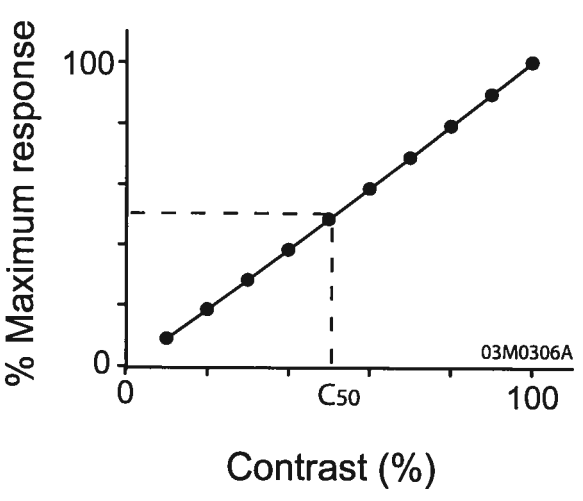
% Maximum response
100
0
0
C50
100
03M0306A
Contrast (%)

form. Optimal contrast levels for the sigmoidal, log, and linear response curves were 0.764 ± 0.271, 0.81 ± 0.145, and 0.922 ± 0.0667 respectively; optimal C_{50} values were 0.565 ± 0.0578, 0.296 ± 0.0786, and 0.482 ± 0.0776, respectively. Panel A depicts a sigmoidal response, where the cell shows minimal response to low contrast, sudden increase at medium contrast, and saturation at high contrast. Panel B shows a logarithmic response with a gradual increase in cell response with increasing contrast levels and a levelling off at high contrast. The final response curve we found was linear (Panel C). The contrast required to evoke a response 50% of the maximum, is defined as the C_{50}. The mean C_{50} for this group was 0.395 ± 0.161. Figure 13 depicts the C_{50} distribution found in normal animals. C_{50} values ranged from 0 to 70% contrast levels. This graph shows that most cells require a high level of contrast to reach half the maximum response.

The mean optimal spatial frequency was low and the mean temporal frequency was high for the normal group. Therefore, in cases where both conditions were optimized, 14 of 16 cells preferred stimuli presented at high speeds (> 10 °/s). The mean optimal speed for the normal group was 209 ± 166 °/s.

3.4.1.5 Cholinergic cells in the retinae of normal rats

The retinae of normal animals were not subject to any immunohistochemistry. It was believed that since these animals did not receive any intravitreal injections, their eyes and retinae would be normal.

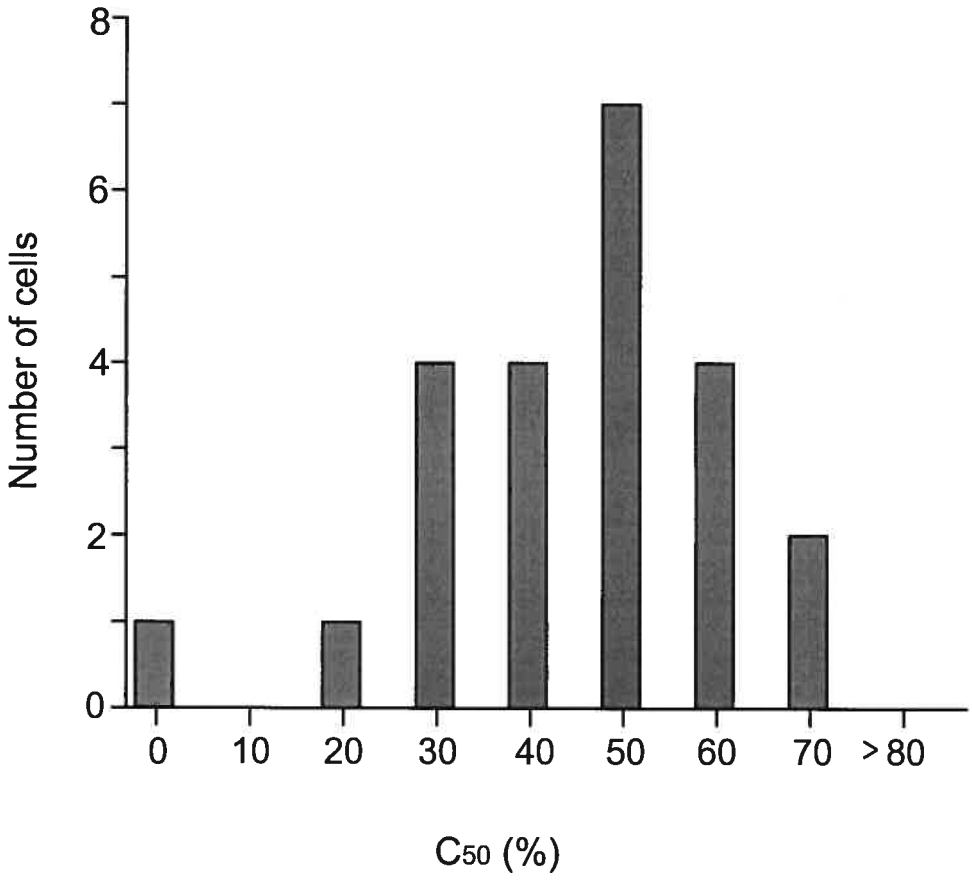

Figure 13: Distribution of C_{50} values from normal animals. C_{50} values ranged from 0 to 70% with a peak at 50% contrast. In most cells of the rat SC, a high contrast level is needed to elicit 50% of the maximum response.

3.4.2 Physiological properties of visual SC neurons in immunotoxin-treated rats

Although the number of visual cells collected from the SC of immunotoxin-treated animals is very small (n = 6), we treated these as preliminary results and made qualitative comparisons with cells from normal animals.

3.4.2.1 Direction selectivity

A total of 6 visual cells were tested in immunotoxin-treated subjects. One cell had no preference and 4 cells were 'orientation' selective. For the 'orientation-selective' neurons, the mean DI was 0.317 ± 0.0912 and none were found to be direction selective. Figure 14 shows a representative example of an 'orientation' selective cell encountered in a treated animal. The cell was selective for 75° and almost equally selective for the opposite direction of 255°. The distribution of the DIs for both normal and toxin-treated rats is presented in figure 15A. The mean bandwidth for immunotoxin-treated rats was $40.1 \pm 16.5°$, similar to that of normal subjects ($48.5 \pm 24°$), as shown in figure 15B.

We also found a multi-unit neuron in the toxin-treated group which we were unable to analyse for direction selectivity. There appeared to be two neurons present that were both 'orientation' selective but not direction selective.

3.4.2.2 Spatial frequency

It would seem that elimination of cholinergic cells from the retina did not affect the SF selectivity in toxin-treated animals. Among the few cells found

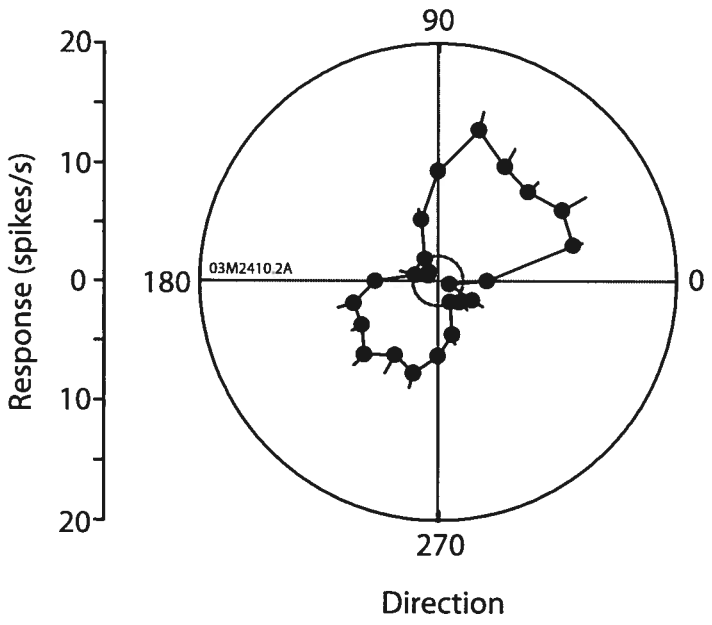

Figure 14: Representative example of an 'orientation' selective cell from a treated subject. The neuron is selective for a direction of 75° and almost equally selective for the grating moving in the opposite direction (255°). Responses are shown as mean ± S.E.M and are represented by solid lines. Dotted lines represent spontaneous activity levels.

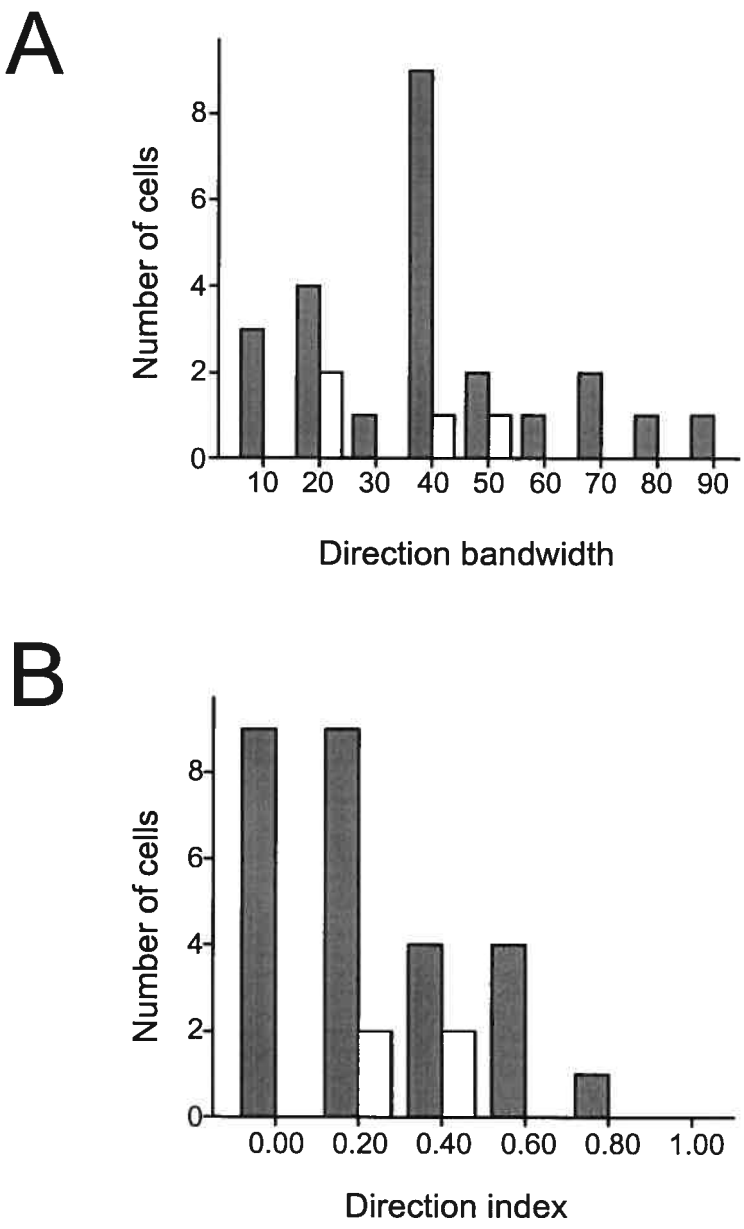

Figure 15: Distribution of DIs and bandwidths of the two groups. **A)** Distribution of DIs in the normal and treated groups, where the mean DI for the normal and treated group is 0.337 ± 0.237 and 0.317 ± 0.0912, respectively. **B)** The broad direction tuned function is represented here by the bandwidth distribution; for normal and treated rats, the mean bandwidth is 48.5 ± 24° and 40.1 ± 16.5°, respectively. Shaded and white columns represent normal and treated animals, respectively.

in the treated group, 2 showed a low pass response profile and 4 were tuned for low frequencies. Neurons with bandpass spatial frequency tuning exhibited a mean bandwidth of 1.2 $\pm$ 1.12 octaves. Representative examples of a lowpass (A) and a tuned (B) are illustrated in figure 16.

The distribution of optimal spatial frequencies for both groups is represented in figure 16C. As aforementioned, the optimal SFs for normal animals ranged from 0.005 to 0.09 c/deg. Mean optimal SF was 0.026 ± 0.26 c/° for the normal group, while the small sample size of the treated animals had a mean optimal SF of 0.026 ± 0.2 c/°. SF for cells from the toxin-treated group ranged from 0.007 to 0.05c/deg.

3.4.2.3 Temporal frequency

All the cells from the treated group exhibited a tuning for low frequencies (n = 6). No major difference was noted in terms of the mean optimal temporal frequency for the normal and treated groups (2.3 $\pm$ 0.99 and 2.7 $\pm$ 0.82 Hz, respectively). The same being true for the mean bandwidth (2.2 $\pm$ 0.71 and 3.0 $\pm$ 1.2 octaves, respectively). Figure 17A depicts a typical example of a temporal frequency response curve found in this group. Figure 17B illustrates the distribution of optimal temporal frequencies for the two groups studied. In the normal group, there were a large proportion of cells which displayed no preference for any TF. However, there was also another proportion that showed a preference for 2 cycles/s. The same preference tendency was noted in the small population of cells found in the toxin-treated subjects.

Figure 16: Response of SC cells to the spatial frequency of drifting gratings from treated rats. **A)** Spatial frequency tuning for a cell with a lowpass response profile. **B)** An example of a bandpass cell tuned for a spatial frequency (0.05 c/°). Responses are shown as mean ± S.E.M and are represented by solid lines. Dotted lines represent spontaneous activity levels. **C)** Distribution of optimal spatial frequencies show cells respond to SFs ranging from 0.005 to 0.09 c/° for normal rats and 0.07 to 0.05 c/°. Shaded and white columns represent normal and treated animals, respectively.

A

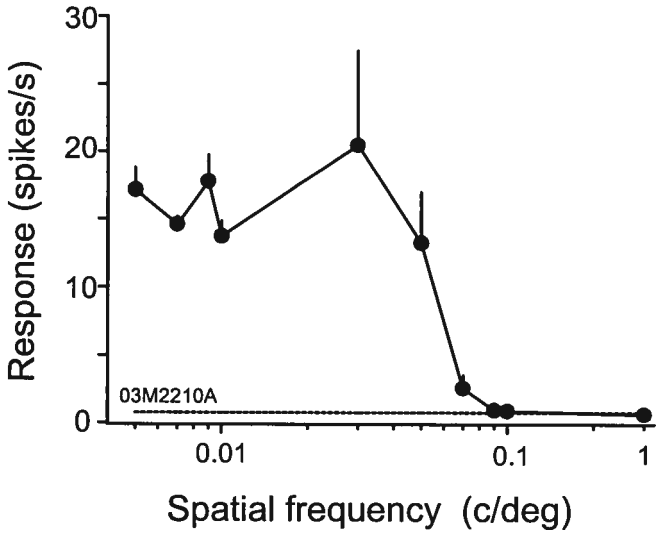
30
20
10
0
Response (spikes/s)
03M2210A
0.01
0.1
1
Spatial frequency (c/deg)

B

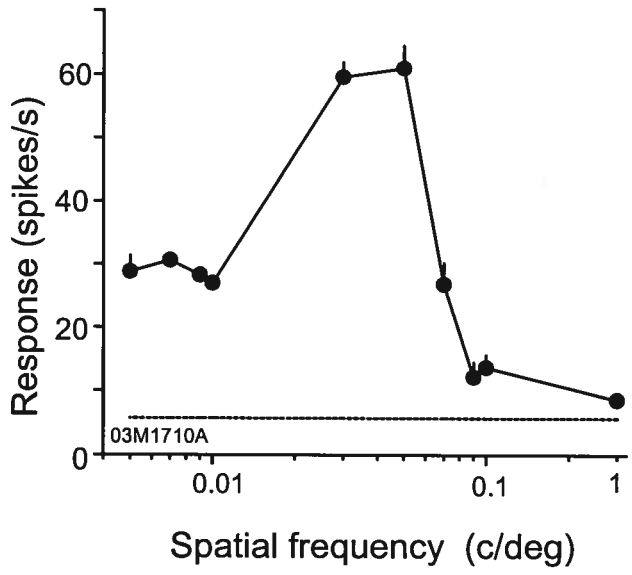
60
40
20
0
Response (spikes/s)
03M1710A
0.01
0.1
1
Spatial frequency (c/deg)

C

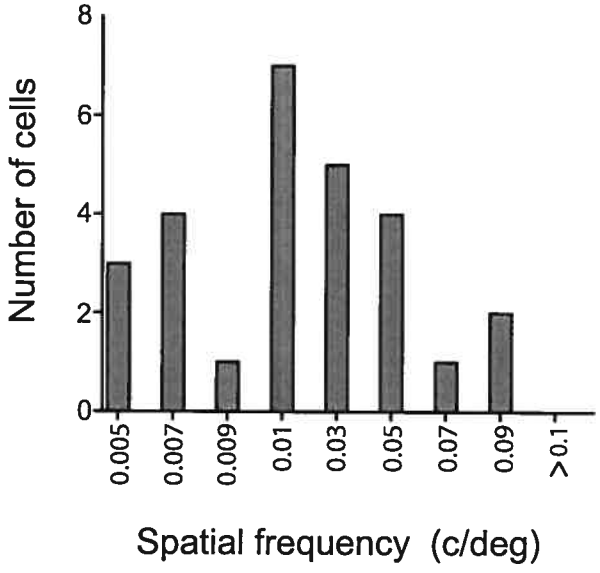
8
6
4
2
0
Number of cells
0.005
0.007
0.009
0.01
0.03
0.05
0.07
0.09
>0.1
Spatial frequency (c/deg)

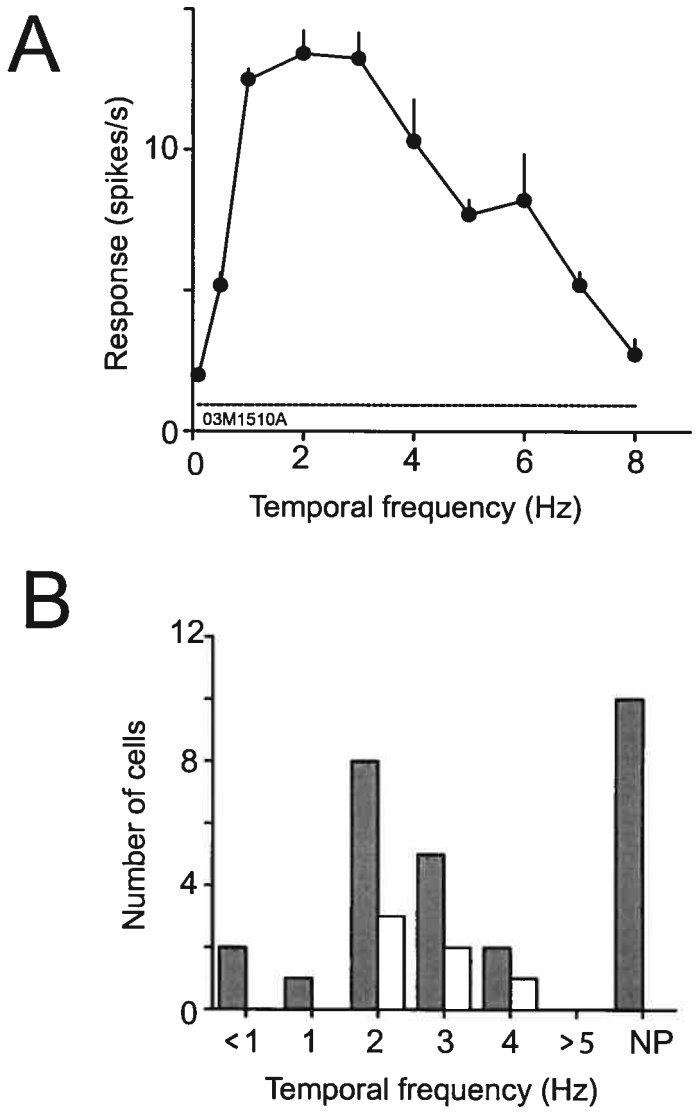

Figure 17: Temporal frequency tuning and distribution of optimal TFs for treated animals. **A)** Illustration of a bandpass cell tuned for 2 Hz. Responses are shown as mean ± S.E.M and are represented by solid lines. The dotted lines represent spontaneous activity levels. **B)** The distribution profile for optimal TFs. The mean optimal TF is 2.7 ± 0.82 Hz. Shaded and white columns represent normal and treated animals, respectively. NP: no preference for a TF.

In both groups, mean optimal spatial frequencies were low and mean temporal frequencies were relatively high. Hence, cells responded selectively to stimuli of high speeds. In the treated animals, all cells showed a preference for high speeds. Accordingly, the mean optimal speed for normal and treated subjects was 209 $\pm$ 166 and 194 $\pm$ 154 °/s, moderately similar for both groups.

3.4.2.4 Contrast selectivity

As was seen for the normal animals, treated subjects also showed an increase in cell response along with stimulus contrast with a mean optimal contrast level of 86.7 $\pm$ 15%. Response curves were either sigmoidal (n = 3), log (n = 1), or linear (n = 2) in form. There were not enough cells in the toxin group to make a significant comparison with the normal animals. Both groups had similar mean C_{50} values (normal: 0.395 $\pm$ 0.161; treated: 0.463 + 0.0545). C_{50} distributions for both normal and treated animals are illustrated in figure 18. The distribution for treated animals followed the same trend noted in the normal group, with cells needing a high contrast level to evoke 50% of the maximum response.

3.4.2.5 Cholinergic cells in immunotoxin-treated retinae

The retinae collected from the animals subject to electrophysiological recordings (n = 5) were then processed. Figure 19 shows cholinergic amacrine cells in the postnatal retina of the rat using an antibody that recognizes a cholinergic-specific marker, ChAT, in a VAChT-saporin immunotoxin-treated and the contralateral untreated eye. In the untreated eye, two distinct bands of

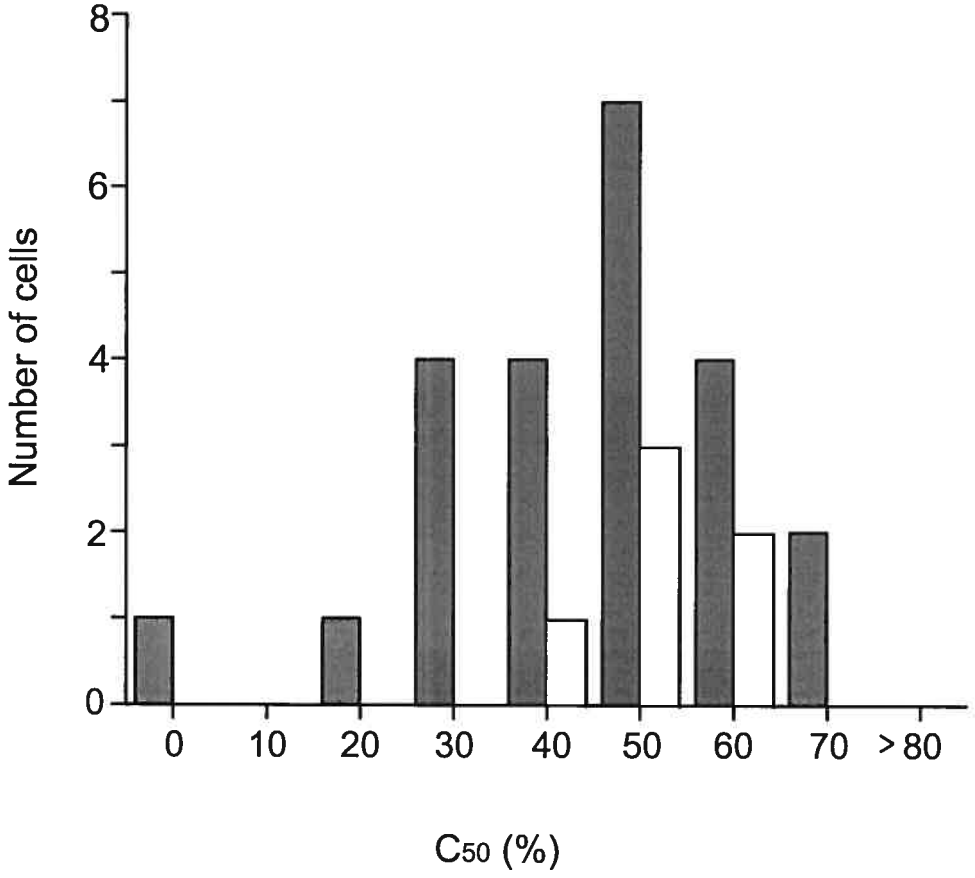

Figure 18: Distribution of C_{50} values from normal and treated animals. C_{50} values ranged from 40 to 60% and 0 to 70% for treated and normal rats, respectively. All cells of both groups required a high contrast level to evoke 50% of the maximum response. Both groups had similar mean C_{50} values (normal: 0.395 $\pm$ 0.161; treated: 0.463 + 0.0545). Shaded and white columns represent normal and treated animals, respectively.

Figure 19: Photomicrographs showing retinal sections of a P1 injected rat processed for ChAT immunohistochemistry at >P60. **A)** ChAT immunoreactivity in cells located in the IPL of the central and peripheral non-treated retina, respectively. **B)** Very weak immunoreactivity is detected in the central and peripheral retina of a P1 toxin-treated animal. GCL: ganglion cell layer; IPL: inner plexiform layer; INL: inner nuclear layer

A

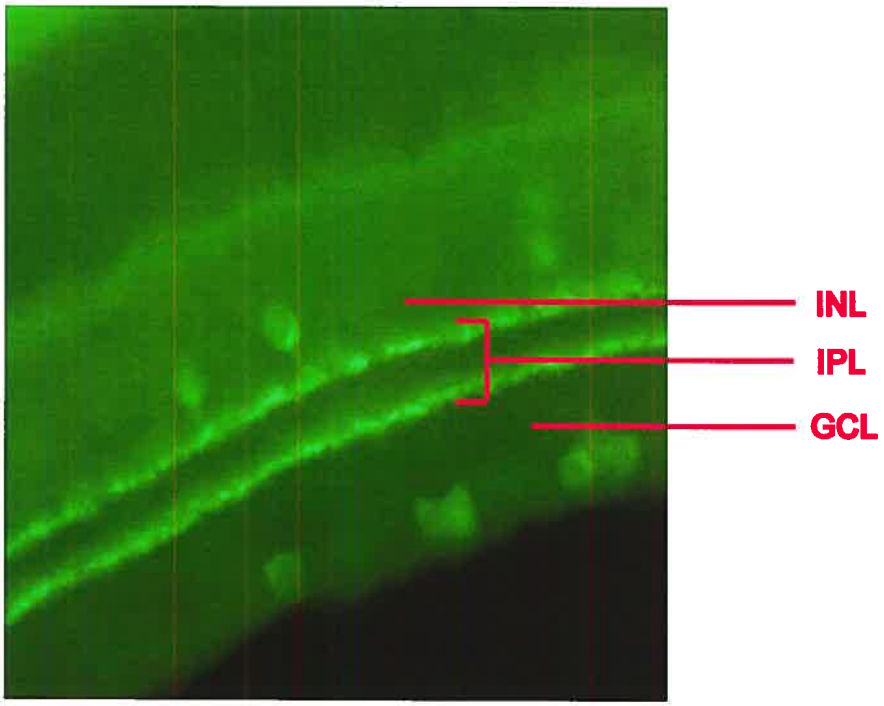

03M0310

B

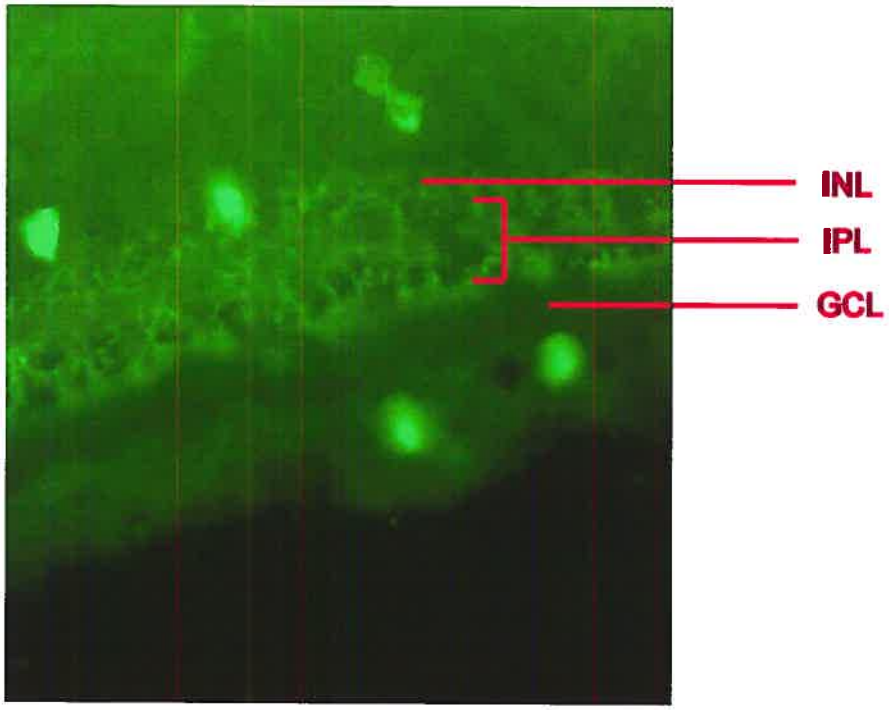

03M0310

0.05 mm

ChAT-immunoreactive processes were observed in the IPL (Figure 19A). Also observed was the soma of two populations of ChAT-immunoreactive cells with strong immunoreactivity in the INL and GCL. The immunotoxin-treated eye displayed some ChAT-immunoreactivity (figure 19B), however, qualitative analysis showed immunoreactivity to be reduced to 50% or less as compared to the untreated eye. Regardless, this was not the expected result as it was hypothesized that the immunotoxin would eliminate all or the majority of cholinergic cells.

Since all treated animals were injected between P1 and P4, the results suggested that P1-P4 was not the most favorable age at which to perform the VAChT-saporin immunotoxin injection since complete elimination of cholinergic neurons was not obtained. Consequently, it was necessary to reveal when was the best time to perform the immunotoxin injection in order to have optimal elimination of cholinergic neurons.

3.5 Histology of SC lesions

Electrolytic lesions were made along all penetrations to allow for a reconstruction of electrode tracks. We were able to reconstruct lesions for 51.4% and 83.3% of penetrations in normal and treated animals, respectively. The majority of electrophysiological recordings done in the SC of both groups were restricted to the SuG (85.7% in normal; 80% in treated), the most dorsal darkest (richest in AChE) layer of the SC. The remaining recordings were done in a more ventral layer, the optic layer (Op).

3.6 General observations on integrity of injected eyes

Once the electrophysiological recordings were completed, both the tested and contralateral eye were removed and compared. In general, if the tested eye had been injected with immunotoxin, it was smaller in diameter when compared to the contralateral eye. At times, the cornea of these eyes had a scratch at the site of injection. The rest of the eye seemed relatively untouched by the injection, with the lens being fully intact. The retina was intact and no detachment from the back of the eye was noted.

3.7 Development of cholinergic neurons at various ages

It has already been established that there is a gradual increase of SA cell expression in the rat retina from E17 till P15 (Kim et al, 2000). We wanted to determine the effect of VAChT-saporin immunotoxin at different developmental stages.

3.7.1 SA cell development one week post-immunotoxin treatment

Salient features in the development of ChAT-immunoreactive cells, determined from microtome cross-sections, are illustrated in figure 20. In all four age groups of rats treated with the immunotoxin (P2, P6, P12, P60; see Table II) no significance difference in the pattern of ChAT immunoreactivity was observed between a normal untreated retina and a toxin-treated retina. The

following description of retinal cholinergic cell development applies for both the normal and toxin-treated eye.

ChAT immunoreactive neurons were present as early as P2 in normal retina. ChAT immunoreactivity was noted in cell bodies in the GCL and the INL, in the central and peripheral retina (Figure 20A and C). It was also observed that there was extensive dendrite arborization of ChAT immunoreactive cells occurring very early in the P2 rat. The same pattern of labeling was present in its counterpart that was immunotoxin-treated (Figure 20B and D).

By P6, ChAT immunoreactive somata were clearly observed in the GCL and INL in all of the normal (Figure 20E and G) and treated (Figure 20H) retinae studied. ChAT immunoreactivity was well distributed in the IPL, with better definition of its inner and outer boundaries.

By P12, the pattern of ChAT immunoreactivity was very similar to that found in mature adult retinae. Present were two populations of ChAT immunoreactive somata evenly distributed on both sides of the IPL, and for the most part, the two parallel bands of dendrites in the IPL were more intensely stained than observed in earlier stages (normal: Figure 20I and K; treated: Figure 20J and K).

The pattern of ChAT immunoreactivity observed in adult retinae was essentially similar to that found in P12 rats, with the exception of a decrease in background staining (normal: Figure 20M and O; treated: Figure 20N and P).

Figure 20: ChAT-immunolabeling of developing cholinergic amacrine cells in cross-sections of central and peripheral regions of the rat retina. Retinae of normal eyes are on the *left*, with toxin-treated retinae on the *right*. Animals were treated at P2, P6, P12 and P60 and their retinae processed 1 week later. From *top* to *bottom*, the images show ChAT-immunolabeling in central and peripheral regions of the retina from normal and treated eyes at P2 (A-D), P6 (E-H), P12 (I-L), and in the adult (M-P). GCL: ganglion cell layer; IPL: inner plexiform layer; INL: inner nuclear layer

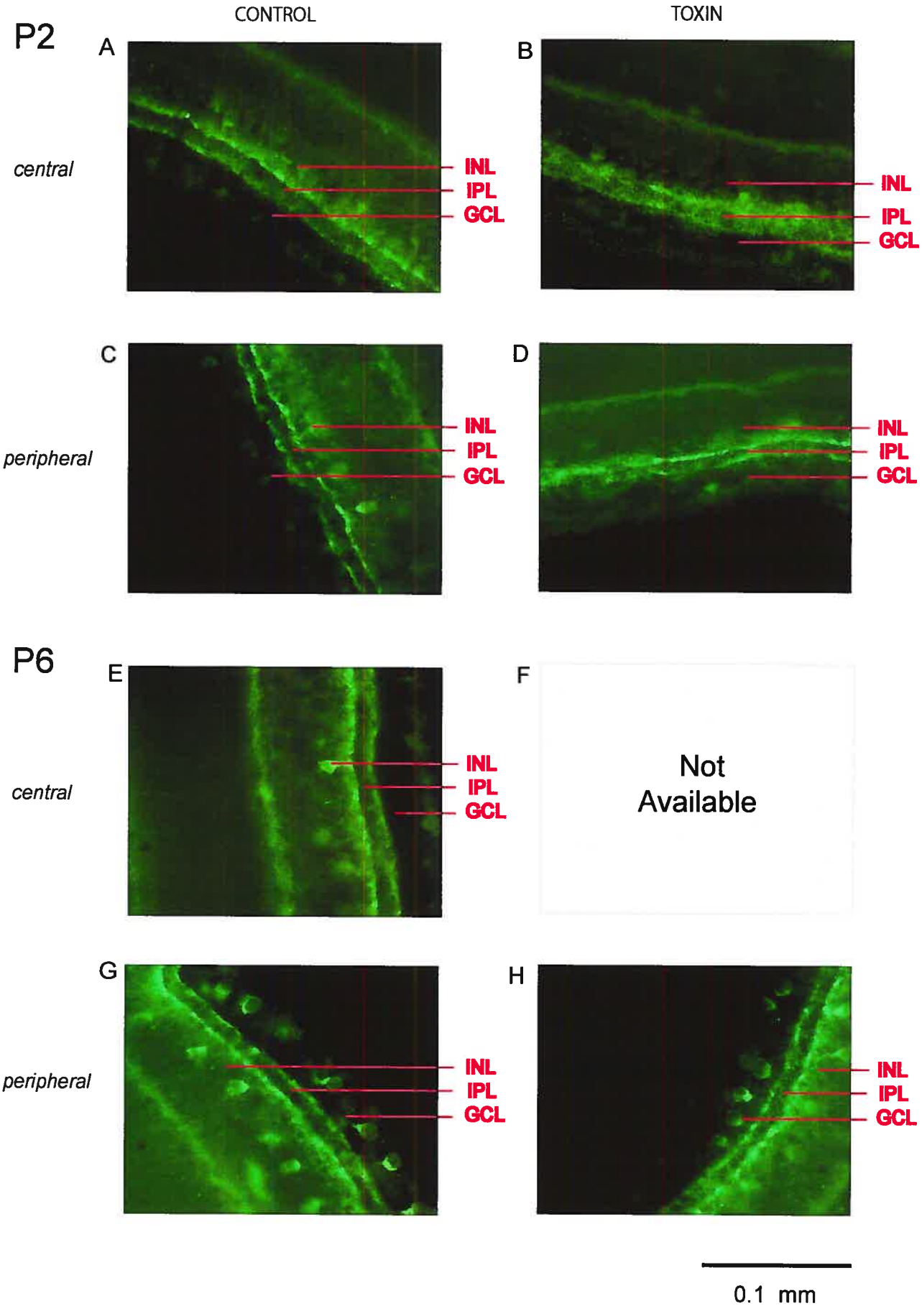
CONTROL
TOXIN
P2
A
B
central
INL
IPL
GCL
INL
IPL
GCL
C
D
peripheral
INL
IPL
GCL
INL
IPL
GCL
P6
E
F
central
INL
IPL
GCL
Not
Available
G
H
peripheral
INL
IPL
GCL
INL
IPL
GCL
0.1 mm

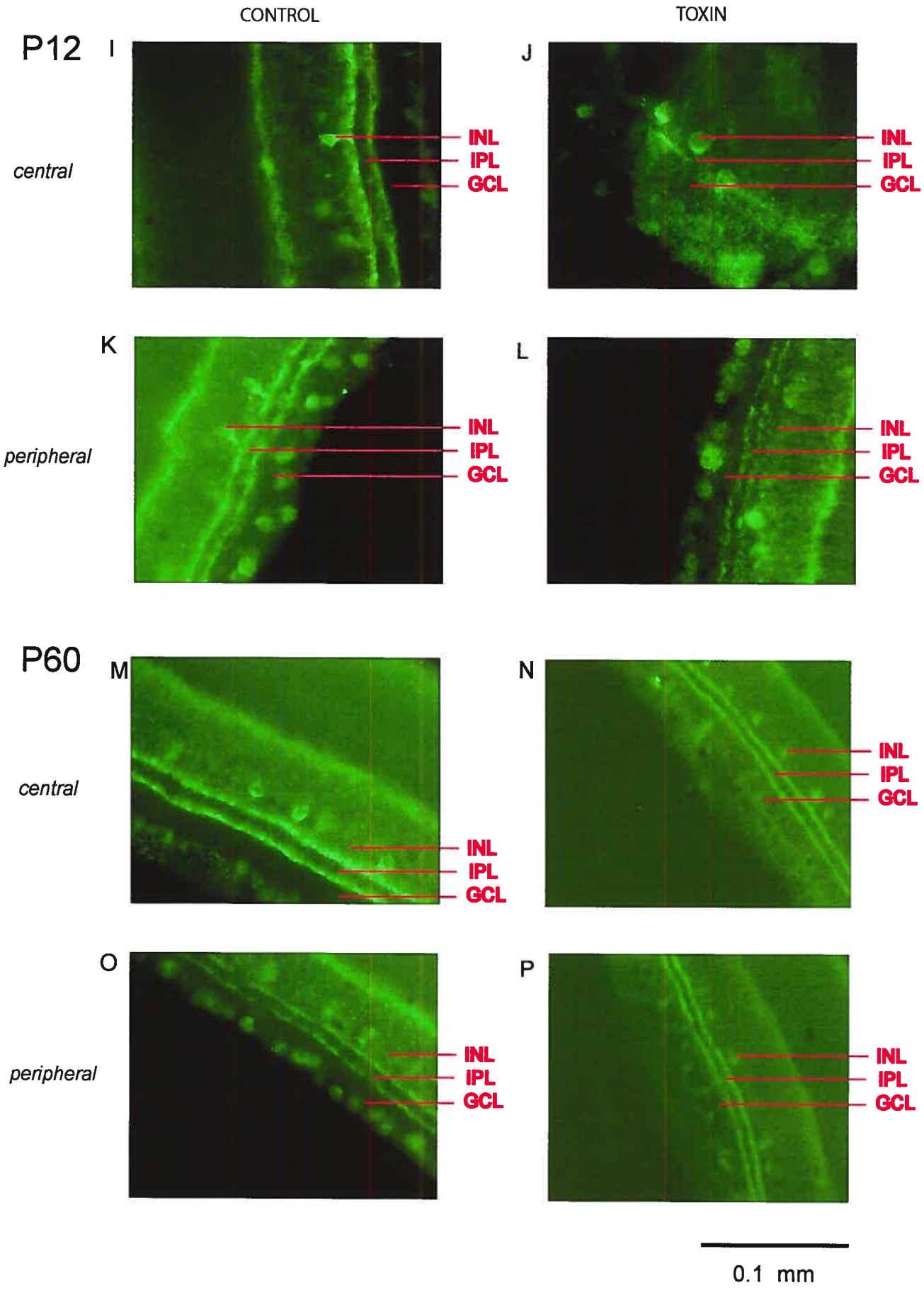
CONTROL
TOXIN
P12
I
J
central
INL
IPL
GCL
INL
IPL
GCL
K
L
peripheral
INL
IPL
GCL
INL
IPL
GCL
P60
M
N
central
INL
IPL
GCL
INL
IPL
GCL
O
P
peripheral
INL
IPL
GCL
INL
IPL
GCL
0.1 mm

DISCUSSION

4.1 Methodological considerations

4.1.1 Intravitreal injections

The protocol for intravitreal injections used in this study had to be completely modified in order to obtain reliable results. The original protocol was supplied by the laboratory of Dr. Chalupa. We used their set-up for our primary injections, and our immunohistochemical results are shown in Appendix I. The results of these injections showed that there was no elimination of cholinergic neurons from the retina. Dr.Chalupa's protocol did not provide a reliable means of injecting precise amounts of the toxin into the eye. There was leakage of the toxin from the syringe even after the needle was removed from the eye. Also, at times, the toxin would be blocked in the syringe. Another major problem with this system was the large size of the needles used to make the pilot-hole (25 gauge) and to perform the intravitreal injection (30 gauge). Consequently, the pilot-hole would be too big once the needle used for the injection was inserted into the eye. This then caused leakage of toxin as well as vitreous humour.

Thus, major modifications were made to the protocol. Firstly, we made the pilot-hole with 31 gauge needles, using a new needle for each penetration; we found that this prevented the use of a blunted-tip for subsequent penetrations. In place of performing injections with a needle, a tapered micropipette was used. This tapered tip created a tight seal with the pilot-hole

and did not allow for outflow of the toxin while the injection was being performed. Finally, all junctions of the syringe-tubing-micropipette system were sealed with epoxy ricin. The system we developed in our lab was very reliable and efficient in delivering the toxin to the eye as compared with the recommended set-up developed by Dr.Chalupa's team.

4.1.2 Anaesthesia

From our study, we determined the best anaesthesia protocol to use with adult rats for electrophysiological recordings in the SC was urethane 1250 – 1500mg/kg at a concentration of 30%, given intraperiteonally. Many studies have used urethane in rats when recording in the SC (Fukuda and Iwama, 1978; Binns and Salt, 1997). We found that this anaesthetic worked very well when the lowest effective dose was given to the rat and overdoses caused rats to die suddenly. Also, if these animals survived until recordings could be performed, brain activity was depressed.

4.2 Justification of the animal model used

There are a number of reasons for choosing rats as subjects in visual experiments. For one, the rat visual system, though not as complex as other mammals, is complicated enough to exemplify important principles of visual function that are not well understood in other mammals. Yet, it is simple enough

to permit those principles to be revealed, and therefore, throw light on many questions pertaining to the visual system. Another reason for the use of rats is its maturity rate. The rat reaches maturity very early as compared to other mammals used in vision studies. Consequently, there is a distinct advantage in using these animals in developmental studies; results can be obtained in a couple of months, rather than years, as with cats or monkeys (Kennedy & Dehay, 1993). It is also worthwhile to note that the rat litter size is relatively large (ranging from 5 to 15 pups), and this permits the researcher to have intra-litter controls.

It is well established that the SC is extremely important for visuomotor integration (Sprague & Meikle, 1965) and orienting behaviour (Goodale & Murison, 1975). The rat is among the mammals whose SC is strongly developed and characterized by a well-organized stratification. Our primary interest in the SC is due to the fact that over 90% of the ganglion cells from the retina have direct projections to the SC (Linden & Perry, 1983). This direct connection is important because it allowed us to determine if the elimination of SA cells would have an effect on the SC neurons' receptive field properties.

4.3 General observations

Our work indicates that P2 injections, while effective in eliminating SA cells in early stages of development, were not effective in eliminating the

majority of SA cells found in adult rat retinae. However, our developmental study was unable to derive any conclusion since the toxin was biochemically ineffective (confirmed by biochemical analysis of the immunotoxin by Dr. L. Chalupa's lab). A further study would be needed to determine which developmental stage is most appropriate for intravitreal injections so there would be complete absence of starburst amacrine cells at the adult stage.

The results also indicated that the volume of immunotoxin injected plays a crucial role in the overall integrity of the eye. Large quantities of immunotoxin were seen to reduce the overall size of the eye and lens, as well, the integrity of the lens was compromised. A possible cause for this eye damage was the substantial increase of intraocular pressure. By reducing the volume of intravitreal injection, we avoided an increase in pressure. This was an important finding since the integrity of the eye was essential for visual stimulation during electrophysiological recordings.

A comparison of receptive field properties of SC neurons from normal and immunotoxin-treated rats was performed. Preliminary results indicate that there is no major difference found between the two groups. However, there are many factors that have to be considered before a definitive conclusion can be made, such as the small population of cells we had in each group.

4.4 Rationale for the use of anti-VAChT-saporin immunotoxin

There have been many other methods used to eliminate cholinergic neurons from the retina. Gómez-Ramos et al (1990) used the AF64A toxin in the mouse, while others have employed immunotoxin-mediated cell targeting (Kobayashi et al., 1995; Yoshida et al., 2001) in transgenic mice, and still yet others have used the immunotoxin 192 IgG-saporin (Pizzo, Waite, Thal, & Winkler, 1999; Yan & Johnson, 1989). However, all these approaches have major drawbacks; the first, causes inflammatory infiltrate and vascular alterations in treated retinae; the second, requires the use of transgenic animals, and therefore, limits the researcher to mice; and the third, is not specific for retinal cholinergic cells as it targets some ganglion and Muller glial cells.

The anti-VAChT-saporin immunotoxin fabricated by Dr. L. Chalupa's laboratory, is specific for retinal cholinergic neurons in the rat and ferret (Gunhan, Choudary, Landerholm, & Chalupa, 2002; Gunhan, van der List, & Chalupa, 2003). Since the target of this toxin is the VAChT and the transporter is found only on cholinergic neurons, it makes this toxin highly specific.

4.5 Short-term development of SA cells after immunotoxin treatment at P1

As aforementioned, the novel immunotoxin was designed to target cholinergic cells. It is internalized only by cholinergic neurons, which then leads to the elimination of amacrine cells by translational arrest of protein synthesis.

Gunhan and colleagues (2002) demonstrated a selective loss of cholinergic amacrine cells from the developing retina. In their study, rat pups had been injected at P1 and euthanized at either P2 or P6. At P2, there was a marked decrease in ChAT-immunoreactivity, and, at P6, there was complete elimination of cholinergic cells. These results were not reflected in our study.

Information from the fabricant of this novel immunotoxin (Dr. L. Chalupa's laboratory) stated that the toxin was stably available for approximately 7 days once injected, and therefore, waiting more than one week post-injection before perform immunohistochemical procedures would not be worthwhile. Thus, six rats received intravitreal injections of the VAChT-saporin immunotoxin at P1. Animals were euthanized one week later and retinae processed. Figure 7 shows the non-treated and immunotoxin-treated retinae from the same rat. The ChAT immunoreactivity was clearly evident in both central and peripheral regions of the non-treated retina. ChAT labelling was most notable within the IPL as two distinct strata of cholinergic processes. Also noted was the labelling of the soma of cholinergic neurons. In contrast, the immunotoxin-treated retina showed a marked decrease in ChAT immunoreactivity with only a few cell bodies labelled. The toxin had an effect for 5 out of the 6 subjects (Figure 7). This result not was expected, since Gunhan and colleagues (2002) noted complete elimination of retinal cholinergic cells at P6 after toxin treatment at P1.

However, we hypothesized that over 90% loss of retinal cholinergic cells was sufficient to begin the electrophysiological recordings, as such a vast amount of the target cells were eliminated.

4.6 Properties of SC neurons

4.6.1 Direction selectivity

Direction selectivity is a property that is generally attributed to cells of the primary visual cortex. However, it is also a property of the SC. The number of direction selective cells found in the SC varies from species to species. To date, there have not been extensive studies done on receptive field properties in the rat. Fukuda and Iwama (1978) found 13.8% of visual cells from the SC were selective for direction, while Gonzalez et al (1992) noted 16% of cells to be direction selective. Studies also show there to be a bias for upward direction. This has also been reported in the mouse (Drager & Hubel, 1975) and golden hamster (Tiao & Blakemore, 1976).

Our findings in the normal rats coincide with the study conducted by Fukuda and Iwama (1978). We found that 12% of our visual cells were direction selective. While Fukuda and Iwama (1978) found direction selective cells to prefer upward motion, we found no common preferred direction of motion within our population of direction-selective cells. This was not surprising given our relatively small sample size (n = 38).

We expected the immunotoxin to eliminate all starburst amacrine cells, and therefore, the cells hypothesized to be crucial for direction selectivity. Thus, in the immunotoxin-treated animals we expected to encounter no direction selective cells, or at least, less of them. In fact, our preliminary results in treated rats showed that there were no direction selective neurons in the SC. However, with a sample population of only five cells, we can hardly state this finding to be significant.

Immunohistochemistry done to the retinae of these animals showed that not all the ChAT-immunoreactive cells were destroyed. Actually, in the majority of cases, approximately 50% of ChAT-immunoreactive somata and dendrites were still present. This could potentially mean that even a sufficient loss of SA cells could be enough to affect the direction selectivity properties of a cell; that is if we take our preliminary results of no direction-selective cells in the treated animals to be representative of all SC cells in treated animals.

4.6.2 Spatio-temporal properties

Thus far, no electrophysiological studies have tried to determine the optimal spatial and temporal frequencies of SC neurons of the rat. There have been behavioural studies done in the rat that indicate the SC can respond to SFs of up to 0.7 c/° (Dean, 1981). Our study found the SF tuning of SC neurons covered a wide range (0.005 to 0.09 c/°), but values never went over 0.09 c/°. With respect to temporal frequency tuning, our results showed that cells prefer

low frequencies in the range of 1 to 3 cycles/s. Similar results for SF were found in the visual cortex of the rat (Girman, Sauve, & Lund, 1999). Girman and colleagues (1999) found the cortex to respond optimally to SFs of 0.08 c/°.

4.6.3 Contrast sensitivity

A large number of animals have been investigated via single cell recordings to determine the contrast response function. Most contrast sensitivity studies performed in the rat have focused on the geniculocortical visual pathway (Powers & Green, 1978; Lennie & Perry, 1981; Silveira, Heywood, & Cowey, 1987). The superior colliculus is a subcortical visual structure that has not been heavily studied in this area.

The results of our study show that there is a clear relationship between stimulus contrast and cell response. The contrast response function demonstrated an increase in cell response with increasing stimulus contrast. This held true for both the normal and toxin-treated animals. We can therefore conclude that cells from the SC of the rat require high stimulus contrast in order to elicit a reliable cellular response. Our findings support prior work done in the rat visual cortex (Shaw, Yinon, & Auerbach, 1975; Waterhouse, Azizi, Burne, & Woodward, 1990; Girman et al., 1999), SC (Humphrey, 1968; Gonzalez, Perez, Acuna, Alonso, & Labandeira-Garcia, 1991), retinal ganglion cells (Powers et al., 1978), and lateral geniculate nucleus (Lennie and Perry, 1981) which found cells responded optimally to contrast levels of greater than 80%. It

could then be said that a common feature of the rat visual system is the requirement of high contrast to trigger a cellular response.

4.7 Developmental course of SA cells

4.7.1 Short-term versus long-term effects of the immunotoxin

To determine if the immunotoxin was an effective in destroying ChAT-immunoreactive cells, we performed injections at P1 and the animals were then sacrificed at P8. We found that ChAT-immunoreactive were almost all eliminated (Figure 7). Thus, we were able to confirm the efficiency of the immunotoxin over short-term development.

Animals from the same litter with the same injection treatment were left to mature until adulthood (> P60) so electrophysiological recordings could then be performed. Immunohistochemistry later revealed that about 50% of ChAT-immunoreactive cells were still present. There are a number of possible explanations for the persistence of cholinergic cells. For one, it is possible that the mechanical damage to the eye (ie. lens and/or ciliary epithelium) during the intravitreal injection caused the release of neurotrophic factors (Fischer, Pavlidis, & Thanos, 2000). However, this is highly unlikely since we took care to inject in the posterior region of the eye and dissection of the eye revealed a fully intact lens.

A second possible explanation for the remaining ChAT-immunoreactivity could be non-specific background staining. This reasoning is highly unlikely since the staining was that of somata and dendrites in regions where SA cells are normally found (IPL, INL and GCL) and no other cholinergic neurons have been found in the retina.

The final reasoning for the persistence of ChAT-immunoreactive cells is the 'birthdate' of starburst amacrine cells. Many studies have focused on the development of retinal cholinergic neurons. As technology becomes more sophisticated, cholinergic cell generation has been detected to begin during earlier stages and end much later in development than once thought. The most recent study performed in rats by Rapaport et al (2004) showed that amacrine cells were formed as early as E14 and their 'birth' ends at about P13. These results coincide with previous research done on the generation of amacrine cells in rats (Kim, Ju, Oh, & Chun, 2000).

Since our injections were done at P1 and the toxin was stably active for one week once the injection was performed, the toxin was not actively available to eliminate SA cells 'born' after P8. It is highly likely that the remaining cholinergic cells we see are cells which were generated after P9. These remaining cells must form between P9 and P13, and therefore, were not affected by the toxin which was inactive by this point. In order to achieve complete elimination of amacrine cells, future studies should perform injection with this immunotoxin after P13 in the rat.

4.7.2 Development of SA cells at various stages of post-natal development

We wanted to investigate the action of the immunotoxin at different stages of development. We performed injections at P2, P6, P12, and P60 and euthanized the rats 1 week later. The results of this study were not what we expected. We found that there was no difference in ChAT-immunoreactivity between the toxin-treated and normal eye (Figure 20). This was most likely due to the ineffectiveness of the immunotoxin. Communications with Dr. L. Chalupa told us that the immunotoxin was in the process of being purified and it was possible that we received an impure batch.

4.8 Conclusions

Our results showed that the immunotoxin was effective in eliminating virtually all cholinergic cells in short-term development, which coincides with prior results found by Gunhan and colleagues (2002, 2003). However, there has been no investigation into the effectiveness of this novel immunotoxin in long-term development. We attempted to answer this question and our study suggests that treatment with anti-VAChT:saporin immunotoxin before too early in development (P2) does not allow for the elimination of retinal cholinergic neurons in long-term development (> P60). Cholinergic cells first appear in the retina at E14 and increase in number till about P12 - P15 (Rapaport, 2004). Therefore, in order to eliminate all cholinergic cells for long-term experiments

where animals are kept until adulthood, injections should be performed anywhere between P12 and P15.

Since SA cells have been implicated to be essential in direction selectivity, we studied electrophysiological properties of the superior colliculus neurons which receive direct efferents from the retina and have comprise a small population of direction selective cells. Investigation of SC neuron properties in normal and treated animals did not demonstrate any significant difference between the two groups. It must be noted that the sample population for both groups was very small.

4.9 Critics and prospectives

One of the major drawbacks for our study was the limited availability of the immunotoxin. This toxin was not commercially available, and therefore, we depended on the laboratory of Dr. L. Chalupa as suppliers of the toxin. At times, we would have to wait months before the toxin was sent to us, and this greatly hindered our progress in this study.

To make reliable comparisons of the treated and normal eye, the same regions of the retina must be compared. In our study, we approximated where the center of the eye was and compared these regions. This method of determining the center of the eye was highly inaccurate. In future studies, it is

recommended to verify the center by determining the diameter of the eye and making a transverse cut through the center of the eye before commencing the embedding procedure required for immunohistochemistry.

Electrophysiological recordings at the adult stage required a fully functional and intact eye. We found that the volume of immunotoxin injected greatly influenced the integrity of the eye. Therefore, all injections were performed with the smallest volume of toxin providing an effective dose.

Finally, results from electrophysiological experiments involved only a small population of cells, especially in the treated group. Subsequent studies would need to increase the sample size so definitive conclusions could be made.

REFERENCES

Amthor, F.R., & Oyster, C.W. (1995). Spatial organization of retinal information about the direction of image motion. Proc Natl Acad Sci U S A, 92(9), 4002-5.

Berman, N., & Cynader, M. (1972). Comparison of receptive-field organization of the superior colliculus in Siamese and normal cats. J Physiol, 224(2), 363-89.

Binns, K.E. & Salt, T.E. (1997). Different roles of GABAA and GABAB receptors in visual processing in the rat superior colliculus. J Physiol, 504 (3), 629-693.

Borg-Graham, L.J. (2001). The computation of directional selectivity in the retina occurs presynaptic to the ganglion cell. Nat Neurosci, 4(2), 176-83.

Brecha, N., Johnson, D., Peichl, L., & Wassle, H. (1988). Cholinergic amacrine cells of the rabbit retina contain glutamate decarboxylase and gamma-aminobutyrate immunoreactivity. Proc Natl Acad Sci U S A, 85(16), 6187-91.

Carter-Dawson, L.D., & LaVail, M.M. (1979). Rods and cones in the mouse retina. II. Autoradiographic analysis of cell generation using tritiated thymidine. J Comp Neurol, 188(2), 263-72.

Chalupa, L.M., & Gunhan, E. (2004). Development of On and Off retinal pathways and retinogeniculate projections. Prog Retin Eye Res, 23(1), 31-51.

Cynader, M., & Berman, N. (1972). Receptive-field organization of monkey superior colliculus. J Neurophysiol, 35(2), 187-201.

Dale, H. (1914). The action of certain esters and ethers of choline, and their relation to muscarine. . J Pharmacol Exp Ther, 6, 147-190.

Dale, H. (1935). Pharmacology and nerve-endings. *Proc R Soc Med* , 28, 319-332.

Daw, N.W., Brunken, W.J., & Parkinson, D. (1989). The function of synaptic transmitters in the retina. Annu Rev Neurosci, 12, 205-25.

Dean, P. (1981). Visual pathways and acuity hooded rats. Behav Brain Res, 3(2), 239-71.

Diao, Y.C., Wang, Y.K., & Xiao, Y.M. (1983). Representation of the binocular visual field in the superior colliculus of the albino rat. Exp Brain Res, 52(1), 67-72.

Dowling JE. (1987a). Retinal cells and information processing. In, The Retina: An approachable part of the brain. (pp. 12-41). Cambridge, MA: Belknap Press.

Dowling JE. (1987b). Approaches to the brain. In, The Retina: An approachable part of the brain. (pp. 1-11). Cambridge, MA: Belknap Press.

Drager, U.C., & Hubel, D.H. (1975). Responses to visual stimulation and relationship between visual, auditory, and somatosensory inputs in mouse superior colliculus. J Neurophysiol, 38(3), 690-713.

Famiglietti, E.V. (1987). Starburst amacrine cells in cat retina are associated with bistratified, presumed directionally selective, ganglion cells. Brain Res, 413(2), 404-8.

Famiglietti, E.V. (1991). Synaptic organization of starburst amacrine cells in rabbit retina: analysis of serial thin sections by electron microscopy and graphic reconstruction. J Comp Neurol, 309(1), 40-70.

Famiglietti, E.V. (1992). Dendritic co-stratification of ON and ON-OFF directionally selective ganglion cells with starburst amacrine cells in rabbit retina. J Comp Neurol, 324(3), 322-35.

Famiglietti, E.V. Jr. (1983). 'Starburst' amacrine cells and cholinergic neurons: mirror-symmetric on and off amacrine cells of rabbit retina. Brain Res, 261(1), 138-44.

Finlay, B.L., Schneps, S.E., Wilson, K.G., & Schneider, G.E. (1978). Topography of visual and somatosensory projections to the superior colliculus of the golden hamster. Brain Res, 142(2), 223-35.

Finlay, B.L., Wilson, K.G., & Schneider, G.E. (1979). Anomalous ipsilateral retinotectal projections in Syrian hamsters with early lesions: topography and functional capacity. J Comp Neurol, 183(4), 721-40.

Fischer, D., Pavlidis, M., & Thanos, S. (2000). Cataractogenic lens injury prevents traumatic ganglion cell death and promotes axonal regeneration both in vivo and in culture. Invest Ophthalmol Vis Sci, 41(12), 3943-54.

Fortin, S., Chabli, A., Dumont, I., Shumikhina, S., Itaya, S.K., & Molotchnikoff, S. (1999). Maturation of visual receptive field properties in the rat superior colliculus. Brain Res Dev Brain Res, 112(1), 55-64.

Fukuda Y, I.K. (1978). Visual receptive-field properties of single cells in the rat superior colliculus.. Jpn J Physiol, 28(3), 385-400.

Girman, S.V., Sauve, Y., & Lund, R.D. (1999). Receptive field properties of single neurons in rat primary visual cortex. J Neurophysiol, 82(1), 301-11.

Goldberg, M.E., & Wurtz, R.H. (1972). Activity of superior colliculus in behaving monkey. I. Visual receptive fields of single neurons. J Neurophysiol, 35(4), 542-59.

Gomez-Ramos, P., Galea, E., & Estrada, C. (1990). Neuronal and microvascular alterations induced by the cholinergic toxin AF64A in the rat retina. Brain Res, 520(1-2), 151-8.

Gonzalez, F., Perez, R., Acuna, C., Alonso, J.M., & Labandeira-Garcia, J.L. (1991). Contrast responses to bright slits of visual cells in the superior colliculus of the albino rat. Int J Neurosci, 58(3-4), 255-9.

Gonzalez, F., Perez, R., Alonso, J.M., Labandeira-Garcia, J.L., & Acuna, C. (1992). Responses of visual single cells in the superior colliculus of the albino rat to bright bars. Arch Ital Biol, 130(4), 249-61.

Goodale, M.A. (1973). Cortico-tectal and intertectal modulation of visual responses in the rat's superior colliculus. Exp Brain Res, 17(1), 75-86.

Goodale, M.A., & Murison, R.C. (1975). The effects of lesions of the superior colliculus on locomotor orientation and the orienting reflex in the rat. Brain Res, 88(2), 243-61.

Graham, J., Berman, N., & Murphy, E.H. (1982). Effects of visual cortical lesions on receptive-field properties of single units in superior colliculus of the rabbit. J Neurophysiol, 47(2), 272-86.

Grun G. (1982). The development of the vertebrate retina: a comparative survey. Adv Anat Embryol Cell Biol, 78, 1-85.

Gunhan, E., Choudary, P.V., Landerholm, T.E., & Chalupa, L.M. (2002). Depletion of cholinergic amacrine cells by a novel immunotoxin does not perturb the formation of segregated on and off cone bipolar cell projections. J Neurosci, 22(6), 2265-73.

Gunhan, E., van der List, D., & Chalupa, L.M. (2003). Ectopic photoreceptors and cone bipolar cells in the developing and mature retina. J Neurosci, 23(4), 1383-9.

Harvey, A.R., & Worthington, D.R. (1990). The projection from different visual cortical areas to the rat superior colliculus. J Comp Neurol, 298(3), 281-92.

Haverkamp, S., Grunert, U., & Wassle, H. (2000). The cone pedicle, a complex synapse in the retina. Neuron, 27(1), 85-95.

Humphrey, N.K. (1968). Responses to visual stimuli of units in the superior colliculus of rats and monkeys. Exp Neurol, 20(3), 312-40.

Huerta M.F. and Harting J.K. (1984). *Comparative neurology of the optic tectum*. NY: Plenum. 687-773 p.

Kadoya, S., Wolin, L.R., & Massopust, L.C. Jr. (1971). Photically evoked unit activity in the tectum opticum of the squirrel monkey. J Comp Neurol, 142(4), 495-508.

Kennedy, H., & Dehay, C. (1993). The importance of developmental timing in cortical specification. Perspect Dev Neurobiol, 1(2), 93-9.

Kim, K.Y., Ju, W.K., Oh, S.J., & Chun, M.H. (2000). The immunocytochemical localization of neuronal nitric oxide synthase in the developing rat retina. Exp Brain Res, 133(4), 419-24.

Kobayashi, K., Morita, S., Sawada, H., Mizuguchi, T., Yamada, K., Nagatsu, I., Fujita, K., Kreitman, R.J., Pastan, I., & Nagatsu, T. (1995). Immunotoxin-mediated conditional disruption of specific neurons in transgenic mice. Proc Natl Acad Sci U S A, 92(4), 1132-6.

Lane, R.H., Allman, J.M., & Kaas, J.H. (1971). Representation of the visual field in the superior colliculus of the grey squirrel (Sciurus carolinensis) and the tree shrew (Tupaia glis). Brain Res, 26(2), 277-92.

Lennie, P., & Perry, V.H. (1981). Spatial contrast sensitivity of cells in the lateral geniculate nucleus of the rat. J Physiol, 315, 69-79.

Linden, R., & Perry, V.H. (1983). Massive retinotectal projection in rats. Brain Res, 272(1), 145-9.

Lund R.D. (1965). Uncrossed visual pathways of hooded and albino rats. Science, 149, 1506-1507.

Masland, R.H., & Mills, J.W. (1979). Autoradiographic identification of acetylcholine in the rabbit retina. J Cell Biol, 83(1), 159-78.

Masland, R. (2003). *The visual neurosciences*. In, Direction selectivity in retinal ganglion cells. (pp. 451-462). Cambridge, MA: MIT Press.

Masland, R. (1986). The cholinergic amacrine cell. TINS, TINS(9), 218-223.

Menger, N., & Wassle, H. (2000). Morphological and physiological properties of the A17 amacrine cell of the rat retina. Vis Neurosci, 17(5), 769-80.

Michael, C.R. (1968). Receptive fields of single optic nerve fibers in a mammal with an all-cone retina. 3. Opponent color units. J Neurophysiol, 31(2), 268-82.

Michael, C.R. (1972). Functional organization of cells in superior colliculus of the ground squirrel. J Neurophysiol, 35(6), 833-46.

Neal, M.J. (1976). Amino acid transmitter substances in the vertebrate retina. Gen Pharmacol, 7(5), 321-32.

O'Malley, D.M., Sandell, J.H., & Masland, R.H. (1992). Co-release of acetylcholine and GABA by the starburst amacrine cells. J Neurosci, 12(4), 1394-408.

Oyster, C.W., & Barlow, H.B. (1967). Direction-selective units in rabbit retina: distribution of preferred directions. Science, 155(764), 841-2.

Palmer, S. (1999). An introduction to vision science. In, Vision Science - Photons to Phenomenology. (pp. 3-42). Cambridge, MA: MIT Press.

Pare, M., Crommelinck, M., & Guitton, D. (1994). Gaze shifts evoked by stimulation of the superior colliculus in the head-free cat conform to the motor map but also depend on stimulus strength and fixation activity. Exp Brain Res, 101(1), 123-39.

Paxinos G., a.W.C. (1997). The rat brain - in stereotaxic coordinates. San Diego, CA: Academic Press.

Pizzo, D.P., Waite, J.J., Thal, L.J., & Winkler, J. (1999). Intraparenchymal infusions of 192 IgG-saporin: development of a method for selective and discrete lesioning of cholinergic basal forebrain nuclei. J Neurosci Methods, 91(1-2), 9-19.

Pourcho, R.G. (1996). Neurotransmitters in the retina. Curr Eye Res, 15(7), 797-803.

Powers, M.K., & Green, D.G. (1978). Single retinal ganglion cell responses in the dark-reared rat: grating acuity, contrast sensitivity, and defocusing. Vision Res, 18(11), 1533-9.

Pycock CJ. (1985). Retinal transmission. Surv Ophthalmol, 29, 355-65.

Rapaport D.H., Wong L.L., Wood E.D., Yasumura D, LaVail M.M. (2004). Timing and topography of cell genesis in the rat retina. J Comp Neurol, 474, 304-24.

Rhoades, R.W., & Chalupa, L.M. (1976). Directional selectivity in the superior colliculus of the golden hamster. Brain Res, 118(2), 334-8.

Rhoades, R.W., & Chalupa, L.M. (1977). Differential effects of stimulus size on "on" and "off" responses of superior collicular neurons. Exp Neurol, 57(1), 57-66.

Rhoades, R.W., & Chalupa, L.M. (1979). Conduction velocity distribution of the retinal input to the hamster's superior colliculus and a correlation with receptive field characteristics. J Comp Neurol, 184(2), 243-63.

Rhoades R.W., Mooney R.D., Fish S.E. (1991). Retinotopic and visuotopic representations in the mammalian superior colliculus. In, Vision and Dysfunction: Neuroanatomy of the Visual Pathways and their Development. (pp. 150-175). Boston: CRC Press.

Rodieck R.W. (1998). Retinas. In, The first steps in seeing. (pp. 36-56). USA: Sinauer Associates, Inc.

Rodieck, R.W., & Marshak, D.W. (1992). Spatial density and distribution of choline acetyltransferase immunoreactive cells in human, macaque, and baboon retinas. J Comp Neurol, 321(1), 46-64.

Schmidt, M., Wassle, H., & Humphrey, M. (1985). Number and distribution of putative cholinergic neurons in the cat retina. Neurosci Lett, 59(3), 235-40.

Schneider G.E. (1969). Two visual systems: Brain mechanisms for localization and discrimination are dissociated by tectal and cortical lesions . Science, 163, 895-902.

Shaw, C., Yinon, U., & Auerbach, E. (1975). Receptive fields and response properties of neurons in the rat visual cortex. Vision Res, 15(2), 203-8.

Sidman, R. (1961). Structure of the eye. In, Histogenesis of the mouse retina studies with thymidine-H3. (pp. 487-506). New York: Academic Press.

Silveira, L.C., Heywood, C.A., & Cowey, A. (1987). Contrast sensitivity and visual acuity of the pigmented rat determined electrophysiologically. Vision Res, 27(10), 1719-31.

Siminoff, R., Schwassmann, H.O., & Kruger, L. (1966). An electrophysiological study of the visual projection to the superior colliculus of the rat. J Comp Neurol, 127(4), 435-44.

Sprague, J.M., & Meikle, T.H. Jr. (1965). The role of the superior colliculus in visually guided behavior. Exp Neurol, 11, 115-46.

Stein, B.E. (1981). Organization of the rodent superior colliculus: some comparisons with other mammals. Behav Brain Res, 3(2), 175-88.

Stein, B.E., & Dixon, J.P. (1979). Properties of superior colliculus neurons in the golden hamster. J Comp Neurol, 183(2), 269-84.

Stein, B.E., & Gaither, N.S. (1981). Sensory representation in reptilian optic tectum: some comparisons with mammals. J Comp Neurol, 202(1), 69-87.

Stein B.E., G.S.J.a.C.H.P. (1976). The control of eye movements by the superior colliculus cells in the cat. Brain Res, 118, 469-474.

Stein BE and Meredith MA. (1991). The functional organization of the superior colliculus. In, The neuronal basis of visual function: vision and visual dysfunction. (pp. 85-110). London, UK: Macmillan.

Sterling, P., & Wickelgren, B.G. (1969). Visual receptive fields in the superior colliculus of the cat. J Neurophysiol, 32(1), 1-15.

Tauchi, M., & Masland, R.H. (1985). Local order among the dendrites of an amacrine cell population. J Neurosci, 5(9), 2494-501.

Taylor, W.R., He, S., Levick, W.R., & Vaney, D.I. (2000). Dendritic computation of direction selectivity by retinal ganglion cells. Science, 289(5488), 2347-50.

Tiao, Y.C., & Blakemore, C. (1976). Functional organization in the superior colliculus of the golden hamster. J Comp Neurol, 168(4), 483-503.

Vaney, D.I. (1994). Territorial organization of direction-selective ganglion cells in rabbit retina. J Neurosci, 14(11 Pt 1), 6301-16.

Vaney, D.I., Peichi, L., & Boycott, B.B. (1981). Matching populations of amacrine cells in the inner nuclear and ganglion cell layers of the rabbit retina. J Comp Neurol, 199(3), 373-91.

Vaney, D.I., & Pow, D.V. (2000). The dendritic architecture of the cholinergic plexus in the rabbit retina: selective labeling by glycine accumulation in the presence of sarcosine. J Comp Neurol, 421(1), 1-13.

Vaney, D.I., & Young, H.M. (1988). GABA-like immunoreactivity in cholinergic amacrine cells of the rabbit retina. Brain Res, 438(1-2), 369-73.

Vaney DI, C.S.Y.H. (1989). Dendritic relationships between cholinergic amacrine cells and direction-selective retinal ganglion cells. In, Neurobiology of the inner retina. (pp. 157-168). Berlin: Springer.

Vaney DI, H.S.T.W.L.W. (2001). Direction-selective ganglion cells in the retina. In, *Motion Vision: Computational, neural, and ecological constraints.* (pp. 13-55). Berlin: Springer.

Vardi, N., Morigiwa, K., Wang, T.L., Shi, Y.J., & Sterling, P. (1998). Neurochemistry of the mammalian cone 'synaptic complex'. Vision Res, 38(10), 1359-69.

Voigt, T. (1986). Cholinergic amacrine cells in the rat retina. J Comp Neurol, 248(1), 19-35.

Waterhouse, B.D., Azizi, S.A., Burne, R.A., & Woodward, D.J. (1990). Modulation of rat cortical area 17 neuronal responses to moving visual stimuli during norepinephrine and serotonin microiontophoresis. Brain Res, 514(2), 276-92.

Weng, S., Sun, W., & He, S. (2005). Identification of ON-OFF direction-selective ganglion cells in the mouse retina. J Physiol, 562(Pt 3), 915-23.

Yan, Q., & Johnson, E.M. Jr. (1989). Immunohistochemical localization and biochemical characterization of nerve growth factor receptor in adult rat brain. J Comp Neurol, 290(4), 585-98.

Yoshida, K., Watanabe, D., Ishikane, H., Tachibana, M., Pastan, I., & Nakanishi, S. (2001). A key role of starburst amacrine cells in originating retinal directional selectivity and optokinetic eye movement. Neuron, 30(3), 771-80.

Young, R.W. (1985a). Cell differentiation in the retina of the mouse. Anat Rec, 212(2), 199-205.

Young, R.W. (1985b). Cell proliferation during postnatal development of the retina in the mouse. Brain Res, 353(2), 229-39.

APPENDIX

Appendix I: Cholinergic amacrine cells in the developed rat retina. The images are vertical sections of adult retinae from a P4 injected rat. The normal (A) and toxin-treated (B) eyes show no difference in ChAT immunoreactivity. Cell bodies are present in the GCL and INL. These is also heavily labeled dendritic processes in the IPL; two sublaminae are clearly labeled. GCL: ganglion cell layer; INL: inner nuclear layer; IPL: inner plexiform layer.

A

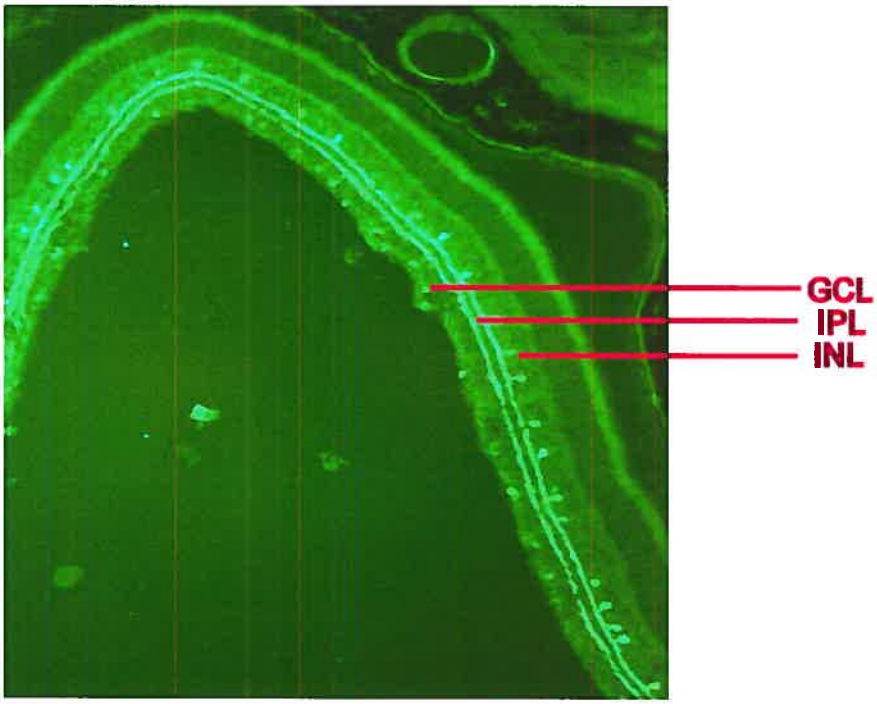

NAM090103

B

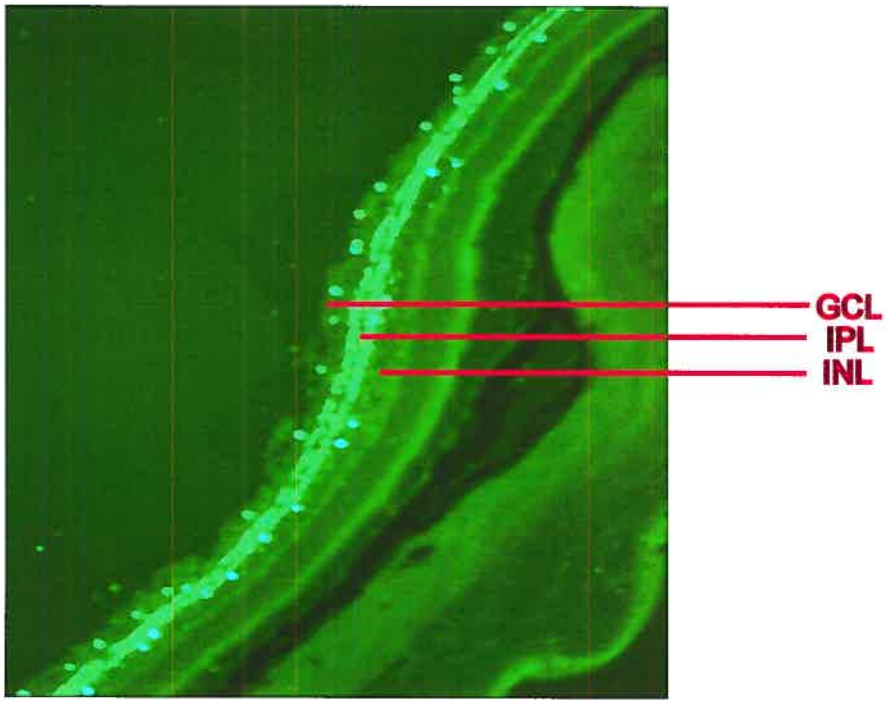

NAM090103

0.1 mm

ACKNOWLEDGEMENTS

ॐ

Firstly, I would like to thank my supervisor, Dr. Christian Casanova, for his understanding and patience, his advice and guidance, and also for his sense of humour during my time in his lab. I would especially like to thank him for all his singing and jokes (that he, at least, found funny). You are a supervisor that is easy to talk to and I thank you for that. The atmosphere in your lab helped me to understand and learn how the scientific world works. You truly made my experience in his lab something I will cherish. Best of luck in the future.

Thank you to Dr. Maurice Ptito for his lively talks and his sense of humour (that you have to love). Thank you to his lab, especially, Dr. Denis Boire, for helping me out when I needed it and introducing me to the wondrous epoxy ricin!

Thanks to Annie-Hélène for her kindness and enthusiasm and for introducing me to Piscine Molitar ;)

Thanks to Brian (a.k.a. Charlie Brown). You have endless patience for my endless questions and my frequent freak-outs when I was in experiment (or even when I wasn't). IRA ≠NRA!!!

Thanks to Éliane, for her friendship and encouragement.....and the look on her face when she walked in on an experiment "en cour"....you're classic ☺.

To Fred, the Master of Perfusions, for his jovial nature and being a human punching bag…how I will miss you. Thanks for all your help.

Thanks to Genevieve, what would I do without you?! You were my partner in crime with my endless surgeries. I will always remember your persuasive nature with the 'mommy' rats that entitled me to leave this lab with all ten fingers fully intact ☺.

To Gino, for his sense of humour, all his electro stories, his advice and those 'HUGE bottles of wine!'. Remember, never accept chewing gum from women from New Orleans….

YOU KNOW Martin, LET'S SAY you had a life, why, who would be around at the lab in the evenings who I could badger with endless electro questions! So, thanks for not having a life and always having an 'encouraging' word and all your insights into the world science and research.

Thanks to Nawal, for being my chocolate supplier (drug dealer) and my French-English dictionary!

Thanks to my parents for supporting and encouraging me throughout my studies.

To my little bro, Roshan, for being my delivery man whenever I forgot my dinner at home.

Finally, thanks to my boyfriend Manny, for his endless support and patience throughout my Master's. Thanks for your late night debates about talking apes, especially those that followed a long day ;) . Your kindness and ability to make me laugh after a long frustrating experiment were very much appreciated. Love you +.